# AGC Kinase Inhibitors Regulate STING Signaling Through SGK-Dependent and SGK-Independent Mechanisms

Johnny Castillo Cabrera[1,2], Hong Dang[3], Zhigang Zhang[2,5], Jose Torres-Castillo[3], Kelin Li[4], Pengda Liu[2,6], Jeff Aubé[4], Blossom Damania[2,5], Robert S. Hagan[3]* and Albert S. Baldwin[2]*

[1]Graduate Curriculum in Pathobiology and Translational Medicine, Biological & Biomedical Sciences Program, UNC School of Medicine, University of North Carolina at Chapel Hill, Chapel Hill, NC, USA; Department of Pathology and Laboratory Medicine, UNC School of Medicine, University of North Carolina at Chapel Hill, Chapel Hill, NC, USA.

[2]Lineberger Comprehensive Cancer Center, UNC School of Medicine, University of North Carolina at Chapel Hill, Chapel Hill, NC, USA.

[3]Division of Pulmonary Diseases and Critical Care Medicine, UNC School of Medicine, University of North Carolina at Chapel Hill, Chapel Hill, NC, USA; Marsico Lung Institute, UNC School of Medicine, University of North Carolina at Chapel Hill, Chapel Hill, NC, USA.

[4]Division of Chemical Biology and Medicinal Chemistry, UNC Eshelman School of Pharmacy, University of North Carolina at Chapel Hill, Chapel Hill, NC, USA.

[5]Department of Microbiology and Immunology, UNC School of Medicine, University of North Carolina at Chapel Hill, Chapel Hill, NC, USA.

[6]Department of Biochemistry and Biophysics, UNC School of Medicine, University of North Carolina at Chapel Hill, Chapel Hill, NC, USA.

*Corresponding authors: robhagan@email.unc.edu and albert_baldwin@med.unc.edu

## Abstract

The STING signaling pathway is essential for the innate immune response to DNA viruses and bacteria and is important in tumor immunity. STING binding to cGAMP or to synthetic agonists leads to the activation of the kinase TBK1 which phosphorylates the transcription factor IRF3 which promotes expression of type 1 interferons such as IFNβ to block viral activity. Aberrant type 1 IFN expression is associated with human diseases including autoimmunity, HIV, and cancer. Here we identify N-[4-(1H-*pyrazolo*[3,4-b] pyrazin-6-yl)-phenyl]-sulfonamide (Sanofi-14h), a compound with preference for inhibition of the AGC family kinase SGK3, as an inhibitor of IFNβ gene expression in response to STING stimulation of macrophages. Sanofi-14h abrogated SGK activity and also impaired activation of the critical TBK1/IRF3 pathway downstream of STING activation, notably blocking the ligand-induced interaction of STING with TBK1. Deletion of SGK1 and SGK3 in macrophages suppressed activation of IFNβ transcription but did not block TBK1/IRF3 activation downstream of STING. Gene and protein expression analysis revealed that deletion of SGK1/3 in a macrophage cell line decreases basal expression of critical transcription factors required for the innate immune response, such as IRF7 and STAT1. Additional studies reveal that other AGC kinase inhibitors block TBK1 and IRF3 activation suggesting common action on a critical regulatory node in the STING pathway. Thus, studies with Sanofi-14h have revealed both SGK-dependent and SGK-independent effects in the STING pathway and suggest a mechanism to alter type 1 IFN transcription through small molecule therapy. (238 words).

64 # Introduction

65

66 Type I interferons (IFNs) are cytokines that play critical roles in the innate immune
67 response by inhibiting viral replication, promoting apoptosis of infected cells, recruiting
68 and activating antigen presenting cells, and eliciting the adaptive immune response
69 through activation of T and B cells[1]. However, dysregulated expression of interferons
70 promotes autoimmune diseases[2], inflammation[3], and immunosuppressive stages of
71 infection[4]. Underscoring the importance of interferons in the immune response, many
72 pathogens express proteins to block interferon production leading to enhanced
73 pathogenicity[5]. Understanding the regulation of IFN expression is critical for elucidating
74 driving events and sequelae in infectious and chronic diseases, and for intervening
75 therapeutically.

76

77 Expression of type I IFNs ($\alpha/\beta$) is induced by stimulation of pathogen receptors including
78 Toll-like receptors (TLR) and nucleic acid receptors such as cGAS[1,6]. In the case of cGAS,
79 binding to cytoplasmic DNA leads to the enzymatic generation of the cyclic dinucleotide
80 2',3' cGAMP[7]. Binding of bacteria- or cGAS-derived cyclic dinucleotides/cGAMP by
81 STING leads to activation of the kinase TANK-binding kinase 1 (TBK1) and to the
82 subsequent phosphorylation of key transcription factors interferon regulatory factor (IRF)
83 3 and 7, which directly promote transcription of type I IFN and other immune response
84 genes[8–11]. Upregulated and secreted type I IFN signals through its receptor (IFNAR) to
85 repress pathogen replication in infected and bystander cells and to activate transcription

86 of a second wave of interferon-stimulated genes (ISGs). ISG expression downstream of
87 IFN requires IFNAR-mediated activation of the JAK-STAT pathway with activating
88 phosphorylation of the STAT1/STAT2/IRF9 (ISGF3) complex as well as STAT3 [12,13] .
89 Multiple layers of regulation by kinases, ubiquitin ligases, and other post-translational
90 modifications tune both the baseline and activation state of the IFN pathway, representing
91 an opportunity for development of chemicals that may repress or restore dysregulated
92 IFN signaling.
93
94 Serum and glucocorticoid-regulated kinases (SGK1-3) are members of the AGC family of
95 serine/threonine kinases with homology to the AKT subfamily[14]. SGK3 is widely
96 expressed, whereas SGK2 expression is restricted largely to the pancreas, brain, kidneys
97 and liver, and SGK1 is expressed in most tissues but with dynamic transcriptional and
98 post-transcriptional regulation[15]. SGK3 uniquely contains a phosphoinositide-binding PX
99 domain at the N-terminus which interacts with phosphatidylinositol-3-phosphate to control
100 SGK3 localization at endosomes[16]. The activation of all three kinases is similar to that for
101 AKT and is controlled by a priming phosphorylation by PI3K/PDK1 and activating
102 phosphorylation by mTORC2[17]. The most well characterized SGK family substrates are
103 members of the N-myc downstream regulated (NDRG) family in addition to several $Na^+/K^+$
104 ion channels [18–22]. All three SGKs are linked to cancer either by promoting drug resistance
105 or by controlling pathways important for cancer progression[15]. Bago et al demonstrated
106 that PI3K/Akt inhibition in breast cancer cells leads to the upregulation of SGK3 to drive
107 mTORC1 activity and tumor growth[23], and Ranzuglia et al proposed SGK2 as regulator

108 of autophagy that modulates platinum drug resistance in cancer cells[24]. SGK1 is the most
109 characterized of the three in cancer with roles in driving tumorigenesis, proliferation,
110 regulation of apoptosis, invasion, metastasis and drug resistance[25].
111
112 SGK inhibition has been proposed as a therapeutic approach in cancer and SGK
113 inhibitors have been developed and tested with this objective[26]. GSK650394, SI113 and
114 EMD638683 are the most widely used inhibitors of SGK in cancer studies and have been
115 shown to block cell proliferation and to decrease tumor growth alone or in combination
116 with other inhibitors in animal models [27–29]. A family of N-[4-(1H-*pyrazolo*[3,4-b] pyrazin-
117 6-yl)-phenyl]-sulfonamides have been described to have more potent and selective
118 inhibitory effects on SGK than previous inhibitors[30]. Furthermore, one derivative of these
119 compounds, named Sanofi-14h, has been used in breast cancer models *in vivo* and *in*
120 *vitro* and in combination with AKT inhibitors [23]. Another derivative (Sanofi-17a) has been
121 studied in a mouse explant model of osteoarthritis[31]. Notably, Sanofi-14h shows higher
122 activity towards SGK3 as compared with SGK1, but also has significant activity against
123 kinases such as S6K1 and MLK3[23]. Sanofi-17a preferentially inhibits SGK1 *in vitro* and
124 has decreased activity against other AGC kinases including SGK3 and S6K[31].
125
126 Studies on the functions of SGK kinases in innate immunity are limited. Reports suggest
127 that SGK1 negatively regulates the TLR4/NF-κB response in mice [32], promotes
128 macrophage polarization to an M1 phenotype[33] , and controls macrophage migration in
129 vascular inflammation[34]. SGK3 was shown to regulate $Ca^{2+}$-mediated dendritic migration

130 in response to lipopolysaccharides (LPS) in mice[35]. SGK1 has been also reported to
131 phosphorylate IKKα at Thr23 and activate NF-κB in Neuro2A cells and to phosphorylate
132 IKKβ(S177A/S181A), but not IKKα, in breast cancer cells to increase NF-κB activity[36,37].
133
134 While testing compounds for effects on IFNβ expression we found that Sanofi-14h impairs
135 IFNβ expression in macrophages downstream of STING. We show here that Sanofi-14h
136 blocks the phosphorylation of TBK1 and IRF3, along with the dimerization and nuclear
137 translocation of IRF3 following treatment with a STING agonist. Deletion of SGK1 and
138 SGK3 in macrophages phenocopies the transcriptional defect of Sanofi-14h-treated cells.
139 However, the SGK1/3-depleted cells retain TBK1 and IRF3 phosphorylation downstream
140 of STING, and Sanofi-14h is able to block TBK1/IRF phosphorylation in SGK1/3-null cells,
141 indicating both SGK-dependent and -independent effects in the response of
142 macrophages to STING activation. Transcription and protein analysis revealed the effect
143 of loss of SGK1 and SGK3 on IFNβ gene expression is through loss of basal expression
144 of several key IRF and STAT family members. Interestingly, Sanofi-14h blocks the
145 recruitment of TBK1 and IRF3 into the STING complex, indicating its ability to block a
146 critical initial step in the STING-TBK1-IRF3 activation pathway. Analysis of other AGC
147 kinase inhibitors across different drug classes revealed that many suppress IRF3
148 activation albeit with different efficacy. These studies indicate unexpected effects of AGC
149 kinase inhibitors on the STING-driven innate immune response with a primary effect at
150 the level of TBK1 and IRF3 activation. Additionally, these studies reveal regulatory effects

151 of SGK1/3 in control of expression of critical transcription factors involved in the innate
152 immune response.

153 # Results

154 **Sanofi-14h blocks IFNβ gene induction induced by STING ligands and HSV-1**

155 While investigating compounds that may affect the induction of IFNβ gene transcription in the
156 STING pathway, we found that N-[4-(1H-*pyrazolo*[3,4-b] pyrazin-6-yl)-phenyl]-sulfonamide
157 (Sanofi-14h) suppressed IFNβ mRNA induction in murine RAW264.7 macrophages treated
158 with DMXAA[38] . The inhibitory response was dose-dependent with a 50% inhibition measured
159 between 500nM and 1μM [**Figure 1A**]. To confirm the biological significance of this response,
160 we analyzed the effect of Sanofi-14h on replication of the dsDNA herpes simplex virus (HSV-
161 1). Consistent with **Figure 1A**, we found that Sanofi-14h increased replication of HSV-1 in
162 RAW264.7 macrophages as measured through plaque-forming assays [**Figure 1B**]. Sanofi-
163 14h also blocked induction of IFNβ mRNA in HSV-1 infected cells [**Figure 1B**].

164 **Sanofi-14h blocks the STING-induced TBK1-IRF3 signaling cascade**

165 STING activation in response to cytoplasmic DNA/viral infection leads to the phosphorylation
166 of the kinase TBK1 which phosphorylates the transcription factor IRF3, leading to its
167 subsequent dimerization and nuclear translocation to promote transcription of the IFNβ gene
168 [13,39]. To determine whether Sanofi-14h affects this signaling pathway, we treated RAW264.7
169 cells with different doses of the inhibitor prior to stimulation with DMXAA. Sanofi-14h pre-

170 treatment led to a dose-dependent inhibition of activating phosphorylation of TBK1, IRF3, and
171 STING [**Figure 1C**]. STING phosphorylation is characterized by the reduction in its
172 electrophoretic mobility. Consistent with the ability of Sanofi-14h to block induction of IFNβ,
173 treatment with this inhibitor led to a marked decrease in STAT3 phosphorylation [**Figure 1C**],
174 which occurs downstream of IFN receptor signaling. We observed that submicromolar doses
175 of Sanofi-14h efficiently blocked phosphorylation of the canonical SGK target NDRG1, while
176 higher doses of Sanofi-14h (>5 μM) potently impaired TBK1 and IRF3 phosphorylation [**Figure**
177 **1C**]. Both SGK1 protein [**Figure 1C**] and mRNA levels [**Suppl. Figure 1A**] are induced by
178 DMXAA treatment and this increase is blocked in a dose-dependent manner by Sanofi-14h.
179 These results indicate that SGK1 is a target gene downstream of STING activation.

180 Additionally, we assayed STING-induced signaling and IFNβ expression in primary mouse
181 bone marrow-derived macrophages (BMDMs) treated with Sanofi-14h. Sanofi-14h efficiently
182 blocks phosphorylation of NDRG1 in BMDMs [**Figure 1C**]. In addition, Sanofi-14h blocked
183 induction of IFNβ mRNA and blocked activating phosphorylation of STAT3, TBK1, and IRF3 in
184 primary macrophage cells [**Figure 1C**].

185 After phosphorylation, IRF3 transcription factor dimerizes and translocates to the nucleus to
186 engage target genes for activation[39]. To further address downstream effects of Sanofi-14h on
187 STING-induced signaling, we measured IRF3 dimerization and nuclear translocation in the
188 presence of the drug following DMXAA stimulation of RAW264.7 cells. We observed that
189 Sanofi-14h inhibited both dimerization and nuclear accumulation of IRF3 in a dose-dependent
190 manner [**Figure 1D**]. Because STAT3 Y705 phosphorylation was blocked by Sanofi-14h, we

191 asked whether this effect was dependent on type 1 IFN expression or via an intrinsic interaction
192 between STAT3 and either SGK1/3 or TBK1. In this regard, TBK1 has been reported to
193 phosphorylate STAT3 at S754 and to modulate its function in the STING pathway in
194 macrophages[40]**.** We co-treated RAW264.7 cells with exogenous IFNβ, DMXAA and Sanofi-
195 14h. We observed that treatment with exogenous IFNβ rescues the STAT3 phosphorylation
196 inhibition in the presence of Sanofi-14h but does not rescue TBK1 phosphorylation inhibition
197 induced by Sanofi-14h [**Figure 1E**]. This result indicates that the loss of p-STAT3 induced by
198 Sanofi-14h is dependent on loss of IFNβ production.

199 **The effects of Sanofi-14h on TBK1/IRF3/STING activation are largely independent of**
200 **SGK1 and SGK3**

201 In RAW264.7 cells, SGK3 is expressed at relatively high levels and SGK1 is expressed at
202 lower levels but is inducible upon STING stimulation [see **Figure 2D**, and **suppl. Fig 1A**].
203 SGK2 is not detected in these cells and is not upregulated with SGK1 or SGK3 knockdown
204 [**Suppl. Figure 1B**]. To determine whether SGK1 and/or 3 are involved in control of IFNβ
205 production and in STING-induced signaling, we generated single and double knockouts (KOs)
206 of SGK1 and SGK3 in RAW264.7 cells using CRISPR-Cas9 [**Figure 2D**]. We then asked
207 whether SGK1/3 KO cells phenocopy cells treated with Sanofi-14h prior to STING agonist
208 treatment. First, we showed that loss of either SGK1 or SGK3 reduced IFNβ mRNA induction
209 following DMXAA treatment [**Figure 2A**]. Next, we analyzed the effect of HSV1 infection on
210 wild-type and SGK1/3 KO cells. RAW264.7 macrophages with single or double deletion of
211 SGK1 or SGK3 showed increased cytopathic effect after HSV-1 infection [**Figure 2B**]. SGK1/3

212 KO macrophages showed an increase in viral proliferation and decreased IFNβ transcription.
213 The effect of SGK3 deletion on IFNβ mRNA was more pronounced than SGK1 deletion, likely
214 reflecting the higher baseline expression of SGK3 protein in RAW264.7 cells [**Figure 2B**]. We
215 generated primary bone marrow-derived macrophages (BMDMs) from SGK3 null mice [41] and
216 infected them with HSV *in vitro*. SGK3 null BMDMs showed increased viral replication as
217 compared with wildtype cells [**Figure 2C**]. Thus, deletion of SGK1/3 in macrophages impairs
218 *in vitro* antiviral defense similar to treatment with Sanofi-14h.

219 We next examined the signaling consequences of SGK deletion in response to DMXAA. We
220 found that SGK3 KO cells demonstrate loss of basal NDRG1 phosphorylation, indicating that
221 in RAW264.7 macrophages SGK3 is the primary NDRG1 kinase [**Figure 2D**]. SGK1 KO, SGK3
222 KO, and dual SGK1/3 KO cells exhibit decreased STAT3 Y705 phosphorylation in response to
223 DMXAA treatment, in agreement with reduced IFNβ expression. Surprisingly, SGK1 KO, SGK3
224 KO, and double KO (dKO) cells have largely intact DMXAA-induced phosphorylation of TBK1
225 and STING [**Figure 2D**]. Consistent with this finding, SGK1/3 KO cells have largely unimpaired
226 IRF3 phosphorylation after STING stimulation [**Figure 2D**]. DMXAA-stimulated dimerization of
227 IRF3 is likewise unaffected by single or dual deletion of SGK1 or SGK3 [**Figure 2E**].
228 Fractionation of the nuclear and cytoplasmic compartments showed reduced nuclear
229 accumulation of phosphorylated STAT3 but not IRF3 in SGK3 KO and SGK1/3 dKO cells
230 [**Figure 2E**]. To test if SGK1/3 KO affects STAT3 through IFN expression or another
231 mechanism, we treated WT and SGK1/3 dKO cells with exogenous IFNβ and found that IFNβ

232 rescues the loss of STAT3 phosphorylation in the dKO cells, indicating that SGK1/3 activate
233 STAT3 via control of IFNβ expression [**Figure 2E**].

234 As indicated in **Figure 2D**, loss of SGK1/3 did not block the phosphorylation of TBK1 or IRF3
235 downstream of DMXAA stimulation, yet Sanofi-14h treatment blocked activation of TBK1 as
236 well as IRF3 in dKO cells [**Figure 2G**]. While knockout of SGK1/3 reduced IFNβ mRNA
237 induction downstream of STING treatment, Sanofi-14h further reduced that response in these
238 cells [**Figure 2G**]. Collectively, these data indicate that Sanofi-14h inhibition of TBK1/IRF3
239 phosphorylation during STING activation is largely independent of SGK1/3 inhibition and that
240 SGK1/3 function through a distinct mechanism to promote STING-induced IFNβ mRNA
241 production.

242 **SGK1 and SGK3 control baseline and inducible expression of innate immune regulators**

243 We next performed RNA sequencing (RNAseq) on WT and SGK1/3 dKO RAW264.7 cells with
244 and without DMXAA stimulation. Unsupervised clustering of unstimulated samples showed
245 clear delineation of WT and SGK-null samples with a large number of genes dysregulated in
246 SGK1/3 KO cells. Gene ontology analysis revealed basal downregulation of genes associated
247 with pattern recognition receptor (PRR) signaling, innate immune response, interferon
248 production, and responses to viral infection in cells lacking SGK1 and SGK3 [**Figure 3A**].
249 These SGK-dependent genes include IFN regulating transcription factors Stat1, Irf7, and Irf9.
250 Volcano plots show SGK-dependent baseline expression of other innate immune genes and
251 Interferon-Stimulated Genes (ISGs) including Ifi44, Il1rn, Usp14, Siglec1, and Oas3.Gene set

252 enrichment analysis (GSEA) comparing dysregulated genes in WT and SGK1/3 dKO cells at
253 baseline indicated loss of gene sets related to host defense with no other strongly significant
254 gene sets identified.

255 We next examined gene expression by RNAseq in STING-activated cells and found striking
256 loss of IFN and ISG pathway genes in SGK1/3 dKO cells stimulated with DMXAA relative to
257 WT cells [**Figure 3B**]. The extent and significance of downregulation is enhanced after DMXAA
258 stimulation relative to the basal state. GSEA confirmed the loss of interferon and host defense
259 pathway transcription in SGK1/3 dKO cells. Other gene sets impacted by SGK1/3 deletion
260 include those involved in antigen processing, T cell stimulation, cell adhesion, and cell
261 differentiation. Examination of individual transcription factors showed that in addition to the
262 baseline defect in expression of Irf1, Irf7, Irf9, Stat2, and Stat6, SGK1/3 dKO macrophages do
263 not upregulate Irf7 or Stat2 RNA after DMXAA treatment [**Figure 3B and 3C**]. We extended
264 these findings by immunoblotting which demonstrated a baseline decrease of STAT1, STAT2,
265 IRF1, IRF7, and IRF9 protein levels in dKO cells [**Figure 3C**]. SGK3 appears to control IRF7,
266 IRF9 and STAT2 preferentially as compared with SGK1. Despite relatively low SGK1 protein
267 expression in RAW264.7 cells, SGK1 KO cells show enhanced loss of IRF4 as compared with
268 SGK3 KO cells. Consistent with the expression defects, we observed that SGK1/3 deletion
269 diminished nuclear translocation of IRF4, IRF9, STAT1 and STAT2 and IRF1 in SGK1/3 KO
270 cells [**Figure 3C**]. IRF9 and STAT1 are part of the Interferon Stimulated Gene Factor 3
271 (ISGF3)[42], which is responsible for inducing expression of Interferon Stimulated Genes (ISGs),
272 IRF1 is also involved in the regulation of ISGs in an IFN dependent and independent manner[43].

273 STAT2 is also part of the ISGF3 complex[42] which partially explains (along with a block in IRF1
274 expression) why the vast majority of affected genes were ISGs. Together, these results
275 indicate that SGK1 and SGK3 regulate the expression of IFNβ and ISGs by controlling
276 expression of innate immune regulators IRF1, IRF4, IRF7, IRF9, STAT1 and STAT2 at the
277 RNA level and prior to STING-induced. Additional immune-related mechanisms could depend
278 on SGK1 and SGK3, both basally and under induced conditions, in macrophages.

279 **Sanofi-14h blocks DMXAA-stimulated Interferon and ISG gene expression in**
280 **macrophages**

281 We next asked whether effects of Sanofi-14h treatment overlap the observed transcriptomic
282 effect of SGK1/3 deletion in RAW264.7 cells. Because high dose (5-10μM) Sanofi-14h
283 efficiently blocks TBK1 activation [**Figure 1C**], we selected a lower dose (500nM) of Sanofi-
284 14h that inhibits SGK1 and SGK3 (as assayed by NDRG1 phosphorylation) but largely leaves
285 TBK1 activation intact. Similar to SGK1/3 deletion, 500nM Sanofi-14h inhibited the inducible
286 expression of Ifnβ1 and Stat1 as well as several ISGs (including Mx1, Gbp5, ISG15, Ifit1/2/3,
287 Rsad2) and chemotaxis-related genes (Ccl5, Cccrl2) [**Figure 3D**]. GSEA analysis confirmed
288 the similar transcriptomic effect of SGK inhibition and deletion, showing that the most affected
289 genes are those related to pathogen sensing. Moreover, RNAseq confirmed that Sanofi-14h
290 at a dose of 500nM has a similar effect as deletion of SGK1 and SGK3 in terms of IFN and
291 ISG expression. However, only Irf1, Stat1 and Stat2 RNA are impaired by Sanofi-14h to a
292 similar level as in SGK dKO cells. Irf7 and Irf9 RNA levels were not significantly reduced by
293 Sanofi-14h during the short (2 h pretreatment, 2 h stimulation) exposure to drug, suggesting

294 they are not wholly responsible for Ifnβ1 regulation by Sanofi-14h in this timeframe[**Figure 3D**].
295 The less broad effect of Sanofi-14h is likely explained by acute responses of the cells versus
296 the stable loss of SGK1/3. These data confirm that Sanofi-14h and SGK1/3 regulate STING-
297 driven gene expression responses in macrophage cells.

298 **Sanofi-14h disrupts STING-stimulated TBK1-STING interaction**

299 In the STING-driven antiviral immune response TBK1 is induced to interact with STING to
300 undergo trans-autophosphorylation, to phosphorylate STING and to activate IRF3[39]. We asked
301 whether doses of Sanofi-14h that inhibit TBK1 activation do so by blocking induced STING-
302 TBK1 interaction. To address this, we pre-treated RAW cells with 5μM Sanofi-14h prior to
303 stimulation with DMXAA followed by co-immunoprecipitation. DMXAA induced robust
304 interaction between STING and TBK1 as expected, and Sanofi-14h efficiently impaired
305 DMXAA induced TBK1-STING interaction [**Figure 4A**]. Additionally, Sanofi-14h blocked
306 DMXAA phosphorylation of STING as indicated by a reduction in the slower migrating STING
307 form [**Figure 4A**][42]. We next examined whether Sanofi-14h treatment alters subcellular
308 trafficking of TBK1 and IRF3 following STING activation. We isolated cytoplasmic and
309 membranous (containing the ER, mitochondria and Golgi) fractions after DMXAA treatment.
310 We observed recruitment and phosphorylation of TBK1 and IRF3 in the membrane fraction as
311 expected [**Figure 4B**]. Pretreatment with Sanofi-14h prior to DMXAA prevented TBK1 and
312 IRF3 translocation/retention and subsequent STING activation in the ER [**Figure 4B**]. These
313 outcomes support the hypothesis that Sanofi-14h inhibits STING pathway signaling by

314 preventing TBK1-STING interaction in the ER, thus blocking subsequent recruitment and
315 phosphorylation of IRF3 and inhibiting this key step in the activation pathway.

316 **Class effects of SGK inhibition on STING/TBK1/IFN signaling**

317 In order to address mechanisms associated with the ability of Sanofi-14h to block the
318 STING/TBK1 activation step downstream of DMXAA treatment, we analyzed other inhibitors
319 of AGC family kinases. Using an IRF3-dependent luciferase reporter system in RAW264.7
320 macrophages (Invivogen), we tested DMXAA-stimulated cells pre-treated with 5 different SGK
321 inhibitors across a 10,000-fold concentration range. For this study we synthesized and tested
322 Sanofi-17a, a structural derivative of Sanofi-14h, that was recently described[31] and which
323 preferentially targets SGK1 over SGK3. We included three other small molecules, namely
324 GSK650394, SI113, and EMD638683, with established SGK inhibitory activity[27–29]. We found
325 that each of these known SGK inhibitors, with the exception of EMD638683, blocked DMXAA-
326 stimulated IRF3-promoter activity with an $IC_{50}$ of 3.334 μM and 5.612 μM, respectively [**Figure**
327 **5A**]. Sanofi-17a was less effective than the other SGK inhibitors in the reporter assay with an
328 $IC_{50}$ of 9.006 μM whereas Sanofi-14h was the most effective with an $IC_{50}$ of 1.728 μM. Since
329 Sanofi-17a is a derivative of Sanofi-14h, we examined the effects of Sanofi-17a on STING-
330 activated signaling. Similar to Sanofi-14h, Sanofi-17a at low micromolar concentrations
331 effectively blocked NDRG1 phosphorylation [**Figure 5B**]. Sanofi-17a inhibited TBK1, STAT3,
332 and IRF3 phosphorylation induced by DMXAA with 50% inhibition of TBK1 phosphorylation
333 seen at ~10μM, similar to but less effective as compared with Sanofi-14h [**Figure 5B and 1C**].

334 It was reported that interaction between the TBK1/STING complex with IRF3 is dependent on
335 the structural activity of P70S6K1[44] without affecting TBK1/STING interaction. In this regard,
336 we examined phosphorylation of ribosomal S6 protein, a substrate of the S6 kinase family,
337 based on reports that P70S6K regulates the STING/TBK1/IRF3 complex[44]. DMXAA stimulated
338 S6 phosphorylation in RAW264.7 cells and this was blocked by Sanofi-17a in the low
339 micromolar range [**Figure 5B**]. Sanofi-17a also impaired DMXAA-stimulated phosphorylation
340 of SGK3 T320 at 500nM [**Figure 5B**]. SGK3 T320 is reported to be a direct phosphorylation
341 substrate of 3-phosphoinositide-dependent protein kinase 1 (PDK1)[45]**.** The sensitivity of SGK3
342 T320 phosphorylation to inhibition by Sanofi-17a may represent either loss of feedback from
343 SGK3 to PDK1 or an undescribed component of SGK3 autophosphorylation at that site. Thus,
344 Sanofi-17a blocks phosphorylation of S6 around 1μM but is less effective at blocking
345 phosphorylation of TBK1 and IRF3.

346 Because SGK inhibitors are reported to have activity against other AGC kinases like P70S6K1
347 or Akt[23], we asked whether the signaling effects of Sanofi-14h treatment overlap with those of
348 Akt or P70S6K inhibitors. In RAW264.7 cells stimulated with DMXAA, Akt inhibition by MK2206
349 or P70S6K inhibition by LY2584702 had no effect on STAT3 Y705 phosphorylation while
350 Sanofi-14h at the same dose completely blocked phospho-STAT3 [**Figure 5B**], consistent with
351 loss of IFNβ production. Akt inhibition had no measurable effect on DMXAA-stimulated
352 phosphorylation of TBK1 or IRF3. P70S6K inhibition partly abrogated IRF3 phosphorylation
353 while leaving TBK1 phosphorylation largely intact, potentially consistent with reports that S6K1
354 interacts with STING[44]**.** When assayed using the IRF3-luciferase reporter, Akt and P70S6K

355 inhibitors had weak effects on reporter activity with $IC_{50}$ greater than 50μM, while Sanofi-14h
356 was significantly more potent [**Figure 5B**]. To further test whether P70S6K inhibition has the
357 same effect as Sanofi-14h we assayed the interaction between TBK1 and STING by co-
358 immunoprecipitation. LY2584702 did not alter the STING-TBK1 interaction after DMXAA
359 treatment [**Figure 5C**], suggesting that Sanofi-14h is unlikely to work by the same mechanism
360 as S6K inhibition. The lack of effect on TBK1 phosphorylation, IFN expression, or STING-
361 TBK1 interaction by Akt or P70S6K inhibitors makes it unlikely that Sanofi-14h affects the
362 TBK1/IFN pathway via those kinases (see Discussion).

363

364 **DISCUSSION**

365 Inhibitors of the SGK family have been developed to target these kinases in cancer as well as
366 other disease indications, such as osteoarthritis. As examples, Bago et al[23] used Sanofi-14h
367 to block induced SGK activity associated with Akt inhibition in breast cancer, and Halland et al
368 [23,31] developed Sanofi-17a to target SGK in an osteoarthritis model. Sanofi-14h is preferential
369 for SGK3 and Sanofi-17a is preferential for SGK1, underscoring the potential importance of
370 SGK subtype preference for these inhibitors related to different biological effects and
371 expression. These studies showed that other kinases are targeted by these inhibitors, as
372 Sanofi-14h was shown to have significant activity against S6K1 and MLK3 [23,31]. Our studies
373 revealed an unexpected effect of Sanofi-14h on inhibition of IFNβ mRNA induction following
374 treatment of macrophages cells with the STING agonist DMXAA (Fig. 1A) and this result was

375 extended to corresponding effects on viral replication and virus-induced IFNβ (Fig. 1B). Sanofi-
376 14h clearly targeted SGK in the macrophage cells as shown through its ability to block
377 phosphorylation of the SGK target NDRG1.

378 To address a mechanism for the inhibition of IFNβ mRNA induction by Sanofi-14h, we analyzed
379 the effects of Sanofi-14h on DMXAA-induced signaling and found this compound blocked
380 phosphorylation of TBK1 and IRF3 as well an IFN-driven STAT3 phosphorylation (Fig. 1C).
381 Notably the effect of blocking of pNDRG1 was nearly complete at a 500nM dose while the
382 inhibitory effects on TBK1 signaling were only partial at that dose, suggesting a different target
383 in controlling TBK1 activation. The effect of Sanofi-14h was shown to be at the level of blocking
384 the induced interaction between STING and TBK1 (Fig. 4), thus at an early stage in the STING-
385 induced signaling pathway (and see below).

386 Analysis of RAW264.7 cells revealed that they express SGK3 at relatively high levels and
387 SGK1 at significantly lower levels. SGK2 expression (RNA and protein) was not detectable in
388 these cells. Interestingly, SGK1 mRNA and protein are induced in the DMXAA-response
389 (Fig.1C and sup 1A), suggesting an important role for SGK1 in the innate immune response
390 as an early response gene. To gain insight into potential mechanisms associated with SGK1/3
391 in the STING-induced pathway, we used CRISPR-CAS9 to knock out expression of these
392 genes in RAW264.7 cells. Consistent with the Sanofi-14h response, loss of SGK1/3 blocked
393 STING-induced IFNβ mRNA induction (Fig. 2A). Yet, loss of SGK1/3 in the macrophage cells
394 did not block the induction of phosphorylation of TBK1 and IRF3, indicating an SGK-
395 independent mechanism for this key regulatory event (Fig. 2D).

396 To gain insight into regulatory roles for SGK1/3 in the STING-induced response, we performed
397 RNA sequencing on the dKO cells at baseline and under DMXAA-stimulated conditions and
398 compared the results to WT cells (Fig. 3). In SGK1/3 KO we found low expression of direct and
399 indirect regulators of IFNβ production IRF1, IRF4, IRF7, IRF9, STAT1 and STAT2 at basal and
400 stimulated conditions at the protein and RNA levels. Among them, IRF7 is essential for the
401 production of IFNβ mRNA in response to STING activation because it directly engages the
402 IFNβ promoter along with IRF3[46]. Like IRF7, other IRFs and STATs were more dependent on
403 SGK3 as shown by their decrease in protein levels in the SGK3 KO cells, whereas IRF4
404 appears dependent on SGK1. Thus, results where loss of SGK1 expression leads to loss of
405 IFNβ expression (Fig. 2B) may be related to the corresponding loss of expression of IRF4, a
406 transcription factor involved in macrophage polarization[47]. IRF1 is essential for the expression
407 of ISGs such as OAS2, BST2 and RNASEL as well as IRF9[43] which along with STAT1 and
408 STAT3 forms a complex termed ISGF3 responsible for IRF7 expression[48] . These results
409 indicate that SGK1 and SGK3 are involved in establishing the expression of a variety of key
410 transcription factors both constitutively and inducible in macrophage cells, thus coordinating
411 the innate immune response.

412 To address whether SGK1/3 play a role in immediate STING-induced signaling, we treated
413 cells with 500nM Sanofi-14h, a dose that is preferential for targeting SGK1/3 over blocking
414 TBK1 activation, and performed RNAseq studies. The results demonstrated that Sanofi-14h
415 blocked expression of a subset of genes within the larger group affected by SGK1 and SGK3
416 knockout such as Irf1, STAT1 and STAT2, which were inhibited prior to STING activation in

417 dKO cells. In comparison, a short pre-treatment with Sanofi-14h did not impair IRF7 or IRF9
418 expression, though these transcripts are under-expressed in SGK KO cells (Fig. 3). This may
419 relate to the short time frame of inhibition compared to CRISPR deletion and to the half-life of
420 Irf7 and Irf9 mRNAs. Likewise, the effects of Sanofi-14h at 500nM were phenotypically similar
421 to those of the dKO cells in terms of the gene sets that were affected after DMXAA treatment.
422 IFNβ production, response to viral cycle, and response to bacterium were among such gene
423 sets. These data suggest that SGK controls expression of IFNβ mRNA by positively regulating
424 IRF7 expression and this may occur via a mechanism involving IRF1, IRF9, STAT1 and STAT2
425 but future experiments will be necessary to define this response.

426 The ability of Sanofi-14h treatment to inhibit activation of TBK1 led us to examine a panel of
427 SGK and AGC family kinase inhibitors for their effects on STING-induced signaling. In this
428 regard, we synthesized Sanofi 17a[31], a derivative of Sanofi-14h, which preferentially targets
429 SGK1 (Fig. 5A)[31]. We found that Sanofi-14h, Sanofi-17a, GSK650394, and SI113 all inhibited
430 STING-driven IRF3 activation in a reporter assay with similar potency. The SGK inhibitor
431 EMD638683, reported to exhibit preference for SGK1 over SGK3 [49], was ineffective at blocking
432 IRF3 activation (Fig. 5A). Sanofi-17a blocked phosphorylation of TBK1 and IRF3, although
433 seemingly less efficiently than Sanofi-14h, with inhibitory effects around 10 μM (Fig. 5B)
434 whereas Sanofi-14h blocks TBK1 and IRF3 in the ~1 μM range (Fig. 1A). Consistently, Sanofi-
435 17a blocked the IRF3-dependent reporter less effectively than did Sanofi-14h (Figure 5A).
436 Overall, our studies show that structurally dissimilar SGK inhibitors such as Sanofi-14h, SI113,
437 and GSK650394 all inhibit the STING-induced innate immune response.

438 It was reported that the AGC family kinase S6K1 associates with STING to promote recruitment
439 of IRF3, but not TBK1, into the STING complex, in the viral-regulated innate immune
440 response[44]. Interestingly, this mechanism was reported to not require the catalytic activity of
441 S6K1. In this regard, we analyzed effects of different AGC kinase inhibitors on phosphorylation
442 of S6 and on the DMXAA-induced downstream signaling response. Sanofi-14h has been
443 shown (in cell-free assays) to block S6K1 in a range similar to that of SGK3 and SGK1[23], while
444 Sanofi 17a was reported to have little to no effect on S6K1 activity [31]. Interestingly, we
445 observed that phosphorylation of S6 is induced by DMXAA (Fig. 5B) suggesting the
446 involvement of an S6 kinase in the STING-induced response. Both Sanofi-17a and Sanofi-14h
447 inhibited the phosphorylation of S6 induced by DMXAA. The Akt inhibitor MK2206 prevented
448 phosphorylation of S6 (though not as effectively as Sanofi-14h) but did not block the induced
449 phosphorylation of TBK1 or IRF3 in the STING pathway. The P70S6K inhibitor LY2584702
450 effectively impeded the induced phosphorylation of S6, but less effectively blocked
451 phosphorylation of IRF3. Consistently neither the Akt inhibitor nor the P70S6K inhibitor affected
452 phosphorylation of STAT3 or activation of the IRF3 reporter. While Sanofi-14h impaired
453 recruitment of TBK1 to the STING complex in response to STING stimulation, LY2584702 did
454 not inhibit recruitment of TBK1 and did not hinder phosphorylation of STING which is controlled
455 by TBK1 recruitment (Fig. 5B). These studies show that S6K and Akt inhibition does not
456 phenocopy SGK inhibition and suggests that Akt and S6K do not mediate the effect of Sanofi-
457 14h and related compounds on TBK1 and IRF3 activation. Our study demonstrates SGK1 and
458 SGK3 as important, targetable regulators of the STING/IFN pathway. Future studies are

459 directed at the mechanism of action of Sanofi-14h, and other SGK/AGC inhibitors, relative to
460 inhibiting TBK1 and IRF3 activation downstream of activated STING.

461 We propose a model in which SGK1/3 control the expression of key regulators of the
462 cGAS/STING pathway (Figure 6). Upon viral infection cGAS recognizes dsDNA and produces
463 2'3'-cGAMP which activates STING, TBK1 then gets recruited to STING in the ER where it
464 phosphorylates IRF3 which subsequently dimerizes and translocates to the nucleus to initiate
465 type I IFNs transcription. TBK1 also phosphorylates IRF7 through an unknown mechanism.
466 Sanofi-14h blocks activation of TBK1 and consequent IRF3 and IRF7 phosphorylation by
467 interacting with a regulator other than SGK1/3. IRF7 protein levels, however, are maintained
468 by SGK1/3 at basal conditions. Either the use of Sanofi-14h or the genetic ablation of SGK1/3
469 renders the cells susceptible to viral infection. This works implicates currently existing SGK
470 inhibitors as useful modulators of IFN signaling and points to the SGK kinase family as a useful
471 target in IFN-related diseases.

472

473 ## Materials and Methods

474 **Cell culture**

475 RAW 264.7 (passage 13), Vero and HEK293T/17(passage 30) cells were purchased from the
476 tissue culture facility at UNC. All cell lines were cultured in DMEM High glucose medium
477 (Gibco, 11995-065) supplemented with 10% fetal bovine Serum (FBS) (Avantor, 97068-085)

478 and 1% penicillin/streptomycin(P/S) (Gibco, 15140122) (regular DMEM) in an atmosphere of
479 5% $CO_2$ and 95% humidity at 37°C. RAW 264.7 cells were maintained in 10 cm plates and
480 passaged with a scraper after reaching 90% confluency from passage 13 until passage 35.
481 DMXAA (Cayman Chemical, 14617) treatments in RAW 264.7 cells were carried out at a 10
482 μg/mL dose for all experiments at a density of $3.5x10^6$ cells in 60 mm plates (immunoblots, RT-
483 qPCR and RNA seq) and $35x10^6$ cells in 10 cm plates (co-IP and cell fractionations).
484 Treatments with Sanofi-14h (MRC Pure Reagents) were performed at the indicated doses.
485 HEK293T/17 cells were maintained in 10 cm plates and passaged after reaching 90%
486 confluency with 2 mL of Trypsin-EDTA (0.25%) (Gibco, 25200056) at 37°C for 2 minutes until
487 passage 50. Cells were regularly tested for mycoplasma. RAW-Dual Lucia (Invivogen, rawd-
488 ismip) cells were maintained in DMEM complemented with 100 μg/mL of Normocin (Invivogen,
489 ant-nr-1), 10% heat inactivated FBS, 200μg/mL of Zeocin (Invivogen, ant-zn-05) and 1%
490 penicillin/streptomycin(P/S). For the luciferase assays RAW-Dual Lucia cells were plated in 96
491 well plates at a density of $0.2x10^6$ cells per well and let to rest until the next morning. Cells
492 were treated with the indicated inhibitors for 2 hours and them stimulated with DMXAA for 24h.
493 The luciferase assay was performed following the manufacturer's instructions.
494

495 **Bone marrow derived macrophages preparation**

496 The SGK3 knockout mice were a kind gift from Dr. David Pearce at the University of California
497 San Francisco and have been described previously[50]. All procedures involving mice handling
498 were in accordance to approved protocols by the University of North Carolina Chapel Hill
499 (IACUC protocol 20-167). Bone marrow from WT and SGK3 KO mice was extracted as

500 previously described [51]. Bone marrow was harvested from mice as previously described[52], and
501 cultured in L929-cell condition media (LCCM) to generate macrophages [53]. Cells were seeded
502 in non-tissue culture treated 10 cm plates (Fisherbrand, FB08755712) in media (complete
503 media) containing RPMI1640(Corning, 10-040-CV), 20% LCCM, 10% FBS, 1%(P/S), 2 mM of
504 L-Glutamine (Gibco, 2503-081), and 55 μM of 2-Mercaptoethanol (Gibco, 21085023). After 24
505 hours cells were washed twice with PBS to remove non-adherent cells and fresh complete
506 media was added. Media was changed on days 3 and 5 prior to scraping, counting, and
507 replating. On day 7 media was changed to regular media without LCCM for 24 hours prior to
508 experiments.
509
510 **Cloning**
511 Guide RNAs targeting mSGK1 exon 5(GATTTCAGGTTCTTCTGGCT) and mSGK3 exon 3
512 (TTCAAGACATTAAATGCAG) were designed using the online tool CHOPCHOP
513 (http://chopchop.cbu.uib.no/) and cloned into TLCV2 (Addgene plasmid # 87360,) as described
514 previously[5455]. Plasmids were transformed into One Shot™ Stbl3™ Chemically Competent *E.*
515 *coli* (Invitrogen, C737303) and plated in ampicillin(100ug/mL) plates overnight at 37°C.
516 Colonies were picked and sequenced using the LNX primer
517 (AGCTCGTTTAGTGAACCGTCAGATC).
518
519 **Lentivirus production**
520 Lentiviral particles were produced as described with some modification[56]. HEK293T/17 cells
521 ($0.75x10^6$ per well) were plated in 6 well plates and after 20 hr cells were co-transfected with

522 the 2μg of TLVC2-gRNA, 1μg of psPAX2 (Addgene #12260) and 0.5μg pMD2.G (Addgene
523 #12259) in a ratio of 4:2:1 using FuGENE HD and OptiMEM according to the manufacturer's
524 instructions. Media was changed the next day and after 48h the viral particles were collected
525 by filtration (0.45 μM filter).
526
527 **CRISPR KO cell line generation**
528 RAW 264.7 cells (passage 13) were plated at a density of $0.75x10^6$ cells per well in a 6 well
529 plates and were infected using 1 mL of lentivirus, 1 mL of fresh regular DMEM, 8μg/mL
530 Polybrene (Santa Cruz Biotechnology, sc-134220) and spin infection (1372 RCF for 1hr at RT).
531 Cells were re-infected the next day and selected the following day with Puromycin(2.5μg/mL).
532 After the non-infected control died a portion of the cells was frozen with BAMBANKER FREEZE
533 freezing media (Fisher Scientific, NC9582225) and the rest was plated in 10 cm without
534 puromycin and supplemented with 1μg/mL of doxycycline which was refreshed every day for
535 7 days. Cells were sorted based their GFP "high" signal and plated in 96 well plates at a ratio
536 of 1 cell/well. Clones were screened for SGK1 or SGK3 KO through immunoblot (Supplemental
537 figure). The double SGK1 and SGK3 KO RAW 264.7 cells were generated by Synthego
538 Corporation (Redwood City, CA, USA) as previously described[57] and single clones were
539 isolated in the same way as the one for the single KOs.
540
541 **Immunoblot**
542 Immunoblots were performed utilizing lysis buffer (50 mM Tris-HCl pH 7.4, 150 mM NaCl, 1mM
543 EDTA, 1mM EGTA, 1 mM Beta-Glycerol-Phosphate, 2.5 mM Sodium-Pyrophosphate, 1%

544 Triton-100X, 0.1% SDS) complemented with fresh protease (Sigma, 11697498001) and
545 phosphatase inhibitors (Sigma, P0044-5ML). Proteins were transferred using the Trans-Blot
546 Turbo RTA Mini 0.2 µm Nitrocellulose Transfer Kit (Bio-Rad, 1704270) in the Trans-Blot Turbo
547 Transfer System (Bio-Rad 1704150). Membranes were then blocked for 1 hat RT in 5% dry
548 milk and blotted with primaries overnight at 4 °C, after three washes with TBST the membranes
549 were blotted with secondary for 1 hat RT in blocking buffer. The three washes were repeated
550 and the membranes were imaged using Clarity Western ECL (Bio-Rad, 1705060) in the
551 ChemiDoc Imaging System. Images were processed with the ImageJ software
552 (https://imagej.nih.gov/ij/). The following primary antibodies were from Cell Signaling
553 Technologies and were used 1:1000 unless otherwise indicated: phospho-STAT3 Thr705
554 (9145S), STAT3 (12640S), phospho-TBK1 Ser172 (5483S), TBK1 (38066S), phospho-IRF3
555 Ser396 (29047S), IRF3 (4302S), STING (50494S), phosphor-NDRG1 Thr346(5482),
556 NDRG1(9408, 1:500), GAPDH (5174S), β-Tubulin(2146S), Lamin A/C (4777), SGK1 (12103),
557 SGK3 (8154), BiP(3177T), STAT1 (14994S), STAT2 (4597S), IRF1 (8478S), IRF4(62834T),
558 IRF7 (72073) and IRF9 (28845S). Anti-Rabbit (W4018) and Anti-Mouse (W4028) secondaries
559 antibodies were bought from Promega.
560

561 **Co-immunoprecipitation**

562 STING immunoprecipitation was performed as previously described [44]. In brief, after treatment
563 samples were lysed in IP buffer (20 mM Tris-HCl pH 7.4, 137 mM NaCl, 1 mM EDTA, 1% NP-
564 40, 10% glycerol) complemented with fresh protease and phosphatase inhibitors. 700 µg of
565 protein were mixed and rotated with 0.5 µg of STING antibody for 3 h at 4 °C after which 25

566 μL of Dynabeads Protein G (Invitrogen, 10004D) were added to each sample and rotated for
567 an additional hour. Samples were washed three times for 5 min with IP buffer at 4 °C. After the
568 last wash, the supernatant was discarded and samples were boiled in 4x loading buffer with
569 10% of 2-Mercaptoethanol for 5 min prior to SDS-PAGE and immunoblotting. Clean-Blot™ IP
570 Detection Reagent (Thermo Fisher, 21230) was used for detection to avoid Ig heavy chain.
571

572 **Nuclear fractionation**

573 Cytoplasmic and nuclear fractions were obtain as previously described[58] with modifications.
574 Cells were washed with PBS and centrifuged at 2,300 RCF for 30 seconds and the supernatant
575 discarded. Cells were resuspended in 250 μL of 0.1% NP-40 diluted in cold PBS (with protease
576 and phosphatase inhibitors) and centrifuged at 4 °C at 2000 RCF for 2 min. The supernatant
577 (cytoplasmic fraction) was removed without disturbing the nuclear pellet. The nuclear pellet
578 was washed by gently resuspending with 1 mL of the 0.1% NP40 buffer and samples were
579 centrifuged for 2 min at 2,000 RCF at 4 °C. The supernatant was discarded and the pellets
580 were resuspended in RIPA buffer and sonicated for 10 min (at high with 30 sec on and 30 Sec
581 off) in a water bath sonicator. After sonication pellets were centrifuged 4 °C at 16, 000 RCF for
582 10 minutes and protein from both fractions were quantified and immunoblotted. β-Tubulin was
583 used as a cytoplasmic control while Lamin A/C was used as nuclear control.
584

585 **ER fractionation**

586 Cytoplasmic and membranous fractionation was performed as previously described[59]. Cells
587 were washed with PBS after treatment, collected and centrifuged at 2, 300 RCF for 30 seconds.

588 The supernatant was removed and cells were resuspended in buffer 1 (200μg/mL Digitonin,
589 150 mM NaCl, 50 mM HEPES pH7.4 (Boston Bioproducts, NC0703855), ddH2O, fresh
590 protease and phosphatase inhibitor) and put on ice for 10 min. Afterwards, they were
591 centrifuged for 2 min at 2000 RCF at 4 °C and the supernatant (cytoplasmic fraction) was
592 removed and the pellets were washed with 1 mL of cold PBS. Pellets were resuspended in
593 buffer 2 (1% NP-40, 150 mM NaCl, 50 mM HEPES pH7.4, ddH2O, fresh protease and
594 phosphatase inhibitor) and left on ice for 30 min. After centrifugation, the supernatant was kept
595 (membranous organelles) and the pellets were discarded. Samples were then quantified and
596 immunoblotted.
597
598 **Dimerization**
599 The IRF3 dimerization procedure was adapted from the literature[60] as follows: after treatment
600 cells collected and lysed in dimerization Buffer (50 mM Tris-HCl pH 7.4, 150 mM NaCl, 1mM
601 EDTA, 1mM EGTA, 1 mM Beta-Glycerol-Phosphate, 2.5 mM Sodium-Pyrophosphate, 1%
602 Triton-100X) for 10 min on ice. Samples were centrifuged for 10 min at maximum speed at 4
603 °C and protein was quantified. Proteins were mixed with 2x native sample buffer (Bio-Rad,
604 1610738) and resolved for 35 min at 200 V in precast gels with native running buffer (25 mM
605 Tris and 192 mM glycine) complemented with 0.2% sodium deoxycholate in the cathode
606 chamber prior to transfer and immunoblotting.
607
608 **Reverse Transcriptase Quantitative PCR (RT-qPCR)**

609 Total RNA was extracted using the Quick-RNA miniprep kit (Zymo Research, R1055). cDNA
610 was prepared with the iScript™ cDNA Synthesis Kit (Bio-Rad, 1708891) and RT-qPCR was
611 performed utilizing the iTaq™ Universal Probes Supermix (Bio-Rad, 1725131) according to the
612 manufacture's instruction. Mouse Taqman probes were ordered from Thermo Fisher: IFNβ
613 (Mm00439552_s1), SGK1 (Mm00441380_m1) and GAPDH (Mm99999915_g1).
614

615 **Herpes Simplex Virus (HSV)**

616 HSV-1 KOS [61] was a kind gift from Dr. Steve Bachenheimer (University Of North Carolina at
617 Chapel Hill) and was expanded as described[62]. Briefly, Vero cells were grown to 100%
618 confluency and infected with HSV (0.01 MOI) in 10 cm plates. 4 days after infection the
619 supernatant was harvested and centrifuged at 700 RCF for 10 min, then 25-30 mL of
620 supernatant was ultracentrifuged in 5 mL of 20% sucrose in sterile $ddH_2O$ (overlayed on the
621 supernatant) at 64, 512 RCF for 3h at 4 °C. The supernatant was discarded and the reminder
622 viral solution was resuspended in PBS to a 1:100 ratio of the original supernatant from the
623 Vero cells infection. The virus was then aliquoted and stored at -80 °C. Viral stocks were titled
624 on Vero cells.
625

626 **HSV infection of RAW 264.7 cells and BMDM**

627 WT and KO RAW 264.7 cells were seeded ($0.45x10^6$ cells/well) in 12 well plates, then infected
628 the next day with 1 mL of DMEM (without serum or P/S) containing HSV KOS (less
629 pathogenetic, yet still infective HSV strain)[63] (MOI 0.1) and left in the incubator for 1h. After
630 this time, the media was replaced with fresh complete DMEM and cells were returned to the

631 incubator. The cell supernatant was collected 24 and 48h after infection, centrifuged for 15 min
632 at 1, 000 RCF and was used to perform a plaque assay in Vero cells as mentioned above. The
633 resulting WT and KO pellets were used for RT-qPCR to determine the expression of IFNβ
634 mRNA. WT RAW 264.7 ($0.25x10^6$ cells/well) were seeded in 12 well plates and treated the day
635 after with 5 μM of Sanofi-14h for 24h. After pre-treatment cells were infected and the plaque
636 assay was performed as described. BMDM were infected in 24 well plates ($0.35x10^6$ cells/well)
637 with HSV (MOI 5) in 300 μL of DMEM for 1h. The media then was replaced with regular RPMI
638 without LCCM, cells were returned to the incubator and after 24h the supernatant was
639 harvested, centrifuged at 1, 972 RCF for 15 min and used to performed the plaque assay.
640

641 **Sanofi-17a synthesis**

642 Compound Sanofi-17a was synthesized according to the reported procedure using trans-1,4-
643 cyclohexanediol instead of mixtures[31]. The final deprotection of THP was performed using
644 HCl in diethyl ether and dichloromethane to minimize the by-product formation using
645 alcoholic solvents. 1 hNMR spectra of Sanofi-17a matched the reported values.
646

647 **RNA sequencing**

648 WT and KO RAW 264.7 cells were plated and treated with DMXAA and Sanofi-14h (0.5 μM)
649 for the indicated times. The RNA was extracted as described and sent to Novogen for
650 sequencing. The details of the strategy used can be found in the supplementary methods.
651

652 **RNA Seq analysis**

653 Paired-end RNA-seq data in FASTQ format were mapped to the mouse reference genome,
654 GRCm39 and Gencode mouse vM27 transcript annotation, using the spliced transcripts
655 alignment to a reference (STAR) software[64]. Gene expression estimates as count of mapped
656 sequence reads, and transcripts per million mapped reads (TPM) were estimated using the
657 transcriptome assembler, StringTie2[65]. Differential gene expression analysis was performed
658 using linear models and the Bioconductor R package, limma, and voom normalization, starting
659 from gene expression count[66,67]. Gene set enrichment analysis were performed on log2
660 transformed fold-changes (logFC) ranks, with the Bioconductor R package, fgsea[68]. Volcano
661 plots and heatmaps were generated using the R package, ggplot2. ggplot2[69] and
662 ComplexHeatmap[70]. Batch-corrected TPMs by ComBat method were obtained using the
663 Bioconductor R package, sva[71], and were used as starting input for the heatmaps. Unless
664 indicated otherwise, the default differentially expressed genes (DEGs) high-lighted in volcano
665 plots and heatmaps were filtered at Benjamini-Hochberg FDR adjusted p-value<0.01, and
666 absolute logFC>1, and average log2 TPM>0.
667
668 **Statistical analysis**
669 GraphPad Prism version 9.0.0 for MAC was used to perform One-way ANOVA followed by
670 Dunnett's multiple comparisons test. Statistical significance was defined by a $P < 0.05$. This
671 software was also use to calculate the inhibitors' $IC_{50}$ values based on the Nonlinear fit function.
672
673
674

## Acknowledgments

We thank the members of the Baldwin and Hagan Lab for their technical and intellectual support. We thank Dr. Matthew McPeek for technical support and Alexia Perryman and Dr. Karel Alcedo for their insightful conversations about this project. This research was supported by the National Institute of Health. Grants: R35-CA197684 and R35-CA197684 to ASB and K08HL143271-01A1 and 1R03HL155249-01 to RSH

## References

1. McNab, F., Mayer-Barber, K., Sher, A., Wack, A. & O'Garra, A. Type I interferons in infectious disease. *Nature Reviews Immunology* **15**, 87–103 (2015).
2. Choubey, D. & Moudgil, K. D. Interferons in autoimmune and inflammatory diseases: Regulation and roles. *Journal of Interferon and Cytokine Research* **31**, 857–865 (2011).
3. Davidson, S., Crotta, S., McCabe, T. M. & Wack, A. Pathogenic potential of interferon αβ in acute influenza infection. *Nature Communications* **5**, (2014).
4. Biron, C. A. Interferons α and β as immune regulators - A new look. *Immunity* **14**, 661–664 (2001).
5. Kim, Y. M. & Shin, E. C. Type I and III interferon responses in SARS-CoV-2 infection. *Experimental and Molecular Medicine* **53**, 750–760 (2021).
6. Wan, D., Jiang, W. & Hao, J. Research Advances in How the cGAS-STING Pathway Controls the Cellular Inflammatory Response. *Frontiers in Immunology* **11**, 1–25 (2020).
7. Ablasser, A. & Chen, Z. J. CGAS in action: Expanding roles in immunity and inflammation. *Science (1979)* **363**, (2019).
8. Sun, L., Wu, J., Du, F., Chen, X. & Chen, Z. J. Cyclic GMP-AMP Synthase Is a Cytosolic DNA Sensor That Activates the Type I Interferon Pathway. *Science (1979)* **339**, 786–791 (2013).
9. Zhang, X., Bai, X. chen & Chen, Z. J. Structures and Mechanisms in the cGAS-STING Innate Immunity Pathway. *Immunity* **53**, 43–53 (2020).
10. Liu, S. *et al.* Phosphorylation of innate immune adaptor proteins MAVS, STING, and TRIF induces IRF3 activation. *Science (1979)* **347**, (2015).
11. Yamashiro, L. H. *et al.* Interferon-independent STING signaling promotes resistance to HSV-1 in vivo. *Nature Communications* **11**, (2020).

12. Mogensen, T. H. IRF and STAT transcription factors - From basic biology to roles in infection, protective immunity, and primary immunodeficiencies. *Frontiers in Immunology* **10**, 1–13 (2019).
13. Barber, G. N. STING-dependent cytosolic DNA sensing pathways. *Trends in Immunology* **35**, 88–93 (2014).
14. Castel, P. *et al.* PDK1-SGK1 Signaling Sustains AKT-Independent mTORC1 Activation and Confers Resistance to PI3Kα Inhibition. *Cancer Cell* **30**, 229–242 (2016).
15. di Cristofano, A. SGK1: The Dark Side of PI3K Signaling. *Current Topics in Developmental Biology* **123**, 49–71 (2017).
16. Guerriero, I., Monaco, G., Coppola, V. & Orlacchio, A. Serum and glucocorticoid-inducible kinase 1 (Sgk1) in nsclc therapy. *Pharmaceuticals* **13**, 1–25 (2020).
17. Pearce, L. R., Komander, D. & Alessi, D. R. The nuts and bolts of AGC protein kinases. *Nature Reviews Molecular Cell Biology* **11**, 9–22 (2010).
18. Villoslada, P. *et al.* Axonal and Myelin Neuroprotection by the Peptoid BN201 in Brain Inflammation. *Neurotherapeutics* **16**, 808–827 (2019).
19. Gasser, J. A. *et al.* SGK3 Mediates INPP4B-Dependent PI3K Signaling in Breast Cancer. *Molecular Cell* **56**, 595–607 (2014).
20. Murray, J. T. *et al.* Exploitation of KESTREL to identify NDRG family members as physiological substrates for SGK1 and GSK3. *Biochemical Journal* **384**, 477–488 (2004).
21. Gamper, N. *et al.* K+ channel activation by all three isoforms of serum- and glucocorticoid-dependent protein kinase SGK. *Pflugers Archiv European Journal of Physiology* **445**, 60–66 (2002).
22. Ahmed, M., Fezai, M., Uzcategui, N. L., Hosseinzadeh, Z. & Lang, F. SGK3 Sensitivity of Voltage Gated K + Channel K v1.5 (KCNA5). *Cellular Physiology and Biochemistry* **38**, 359–367 (2016).
23. Bago, R. *et al.* The hVps34- SGK 3 pathway alleviates sustained PI3K/Akt inhibition by stimulating mTORC 1 and tumour growth . *The EMBO Journal* **35**, 1902–1922 (2016).
24. Ranzuglia, V. *et al.* Serum- and glucocorticoid- inducible kinase 2, SGK2, is a novel autophagy regulator and modulates platinum drugs response in cancer cells. *Oncogene* **39**, 6370–6386 (2020).
25. Sang, Y. *et al.* SGK1 in Human Cancer: Emerging Roles and Mechanisms. *Frontiers in Oncology* **10**, 1–17 (2021).
26. Basnet, R., Gong, G. Q., Li, C. & Wang, M. W. Serum and glucocorticoid inducible protein kinases (SGKs): a potential target for cancer intervention. *Acta Pharmaceutica Sinica B* **8**, 767–771 (2018).
27. Liang, X. *et al.* Development of a new analog of SGK1 inhibitor and its evaluation as a therapeutic molecule of colorectal cancer. *J Cancer* **8**, 2256–2262 (2017).
28. Towhid, S. T. *et al.* Inhibition of colonic tumor growth by the selective SGK inhibitor EMD638683. *Cellular Physiology and Biochemistry* **32**, 838–848 (2013).
29. D'Antona, L. *et al.* SI113, a specific inhibitor of the Sgk1 kinase activity that counteracts cancer cell proliferation. *Cellular Physiology and Biochemistry* **35**, 2006–2018 (2015).

30. Halland, N. *et al.* Discovery of N-[4-(1H-pyrazolo[3,4-b]pyrazin-6-yl)-phenyl]-sulfonamides as highly active and selective SGK1 inhibitors. *ACS Medicinal Chemistry Letters* **6**, 73–78 (2015).
31. Halland, N. *et al.* Rational Design of Highly Potent, Selective, and Bioavailable SGK1 Protein Kinase Inhibitors for the Treatment of Osteoarthritis. *Journal of Medicinal Chemistry* (2021) doi:10.1021/acs.jmedchem.1c01601.
32. Zhou, H. *et al.* Inhibition of serum-and glucocorticoid-inducible kinase 1 enhances TLR-mediated inflammation and promotes endotoxin-driven organ failure. *FASEB Journal* **29**, 3737–3749 (2015).
33. Ren, J. *et al.* Serum- and Glucocorticoid-Inducible Kinase 1 Promotes Alternative Macrophage Polarization and Restrains Inflammation through FoxO1 and STAT3 Signaling. *The Journal of Immunology* **207**, 268–280 (2021).
34. Borst, O. *et al.* Pivotal role of serum- and glucocorticoid-inducible kinase 1 in vascular inflammation and atherogenesis. *Arteriosclerosis, Thrombosis, and Vascular Biology* **35**, 547–557 (2015).
35. Schmid, E. *et al.* SGK3 Regulates Ca 2+ Entry and Migration of Dendritic Cells. *Cellular Physiology and Biochemistry* **30**, 1423–1435 (2012).
36. Tai, D. J. C., Su, C. C., Ma, Y. L. & Lee, E. H. Y. SGK1 phosphorylation of IκB kinase α and p300 up-regulates NF-κB activity and increases N-methyl-D-aspartate receptorNR2A and NR2B expression. *Journal of Biological Chemistry* **284**, 4073–4089 (2009).
37. Zhang, L., Cui, R., Cheng, X. & Du, J. Antiapoptotic effect of serum and glucocorticoid-inducible protein kinase is mediated by novel mechanism activating IκB kinase. *Cancer Research* **65**, 457–464 (2005).
38. Prantner, D. *et al.* 5,6-Dimethylxanthenone-4-acetic acid (DMXAA) activates stimulator of interferon gene (STING)-dependent innate immune pathways and is regulated by mitochondrial membrane potential. *Journal of Biological Chemistry* **287**, 39776–39788 (2012).
39. Hopfner, K. P. & Hornung, V. Molecular mechanisms and cellular functions of cGAS–STING signalling. *Nature Reviews Molecular Cell Biology* **21**, 501–521 (2020).
40. Hsia, H. C., Hutti, J. E. & Baldwin, A. S. Cytosolic DNA promotes signal transducer and activator of transcription 3 (STAT3) phosphorylation by TANK-binding kinase 1 (TBK1) to restrain STAT3 activity. *Journal of Biological Chemistry* **292**, 5405–5417 (2017).
41. Grahammer, F. *et al.* Renal function of gene-targeted mice lacking both SGK1 and SGK3. *American Journal of Physiology - Regulatory Integrative and Comparative Physiology* **290**, 945–950 (2006).
42. Tsai, M. H., Pai, L. M. & Lee, C. K. Fine-tuning of type I interferon response by STAT3. *Frontiers in Immunology* **10**, 1–10 (2019).
43. Panda, D. *et al.* IRF1 maintains optimal constitutive expression of antiviral genes and regulates the early antiviral response. *Frontiers in Immunology* **10**, 1–16 (2019).
44. Wang, F. *et al.* S6K-STING interaction regulates cytosolic DNA-mediated activation of the transcription factor IRF3. *Nature Immunology* **17**, 514–522 (2016).

793 45. Bruhn, M. A., Pearson, R. B., Hannan, R. D. & Sheppard, K. E. AKT-independent PI3-
794 K signaling in cancer - Emerging role for SGK3. *Cancer Management and Research* **5**,
795 281–292 (2013).
796 46. Ning, S., Pagano, J. S. & Barber, G. N. IRF7: Activation, regulation, modification and
797 function. *Genes and Immunity* **12**, 399–414 (2011).
798 47. Sasaki, K. *et al.* Deletion of myeloid interferon regulatory factor 4 (Irf4) in mouse model
799 protects against kidney fibrosis after ischemic injury by decreased macrophage
800 recruitment and activation. Journal of the American Society of Nephrology vol. 32 (2021).
801 48. Platanitis, E. et al. A molecular switch from STAT2-IRF9 to ISGF3 underlies
802 interferon-induced gene transcription. *Nature Communications* **10**, 1–17 (2019).
803 49. Ackermann, T. F. *et al.* EMD638683, a Novel SGK Inhibitor with Antihypertensive
804 Potency. *Cellular Physiology and Biochemistry* **28**, 137–146 (2011).
805 50. McCormick, J. A. *et al.* Targeted Disruption of the Protein Kinase SGK3/CISK Impairs
806 Postnatal Hair Follicle Development. *Molecular Biology of the Cell* **15**, 4278–4288
807 (2004).
808 51. Marim, F. M., Silveira, T. N., Lima, D. S. & Zamboni, D. S. A Method for Generation
809 of Bone Marrow-Derived Macrophages from Cryopreserved Mouse Bone Marrow Cells.
810 *PLoS ONE* **5**, 1–8 (2010).
811 52. Zamboni, D. S. & Rabinovitch, M. Nitric oxide partially controls Coxiella burnetii
812 phase II infection in mouse primary macrophages. *Infection and Immunity* **71**, 1225–1233
813 (2003).
814 53. Englen, M. D., Valdez, Y. E., Lehnert, N. M. & Lehnert, B. E. Granulocyte/macrophage
815 colony-stimulating factor is expressed and secreted in cultures of murine L929 cells.
816 *Journal of Immunological Methods* **184**, 281–283 (1995).
817 54. Sanjana #1, N. E., Shalem #1, O. & Zhang, F. Improved vectors and genome-wide
818 libraries for CRISPR screening HHS Public Access Supplementary Material. *Nat Methods*
819 **11**, 783–784 (2014).
820 55. Boukhaled, G. M., Harding, S. & Brooks, D. G. Opposing Roles of Type I Interferons in
821 Cancer Immunity. *Annual Review of Pathology: Mechanisms of Disease* **16**, 167–198
822 (2021).
823 56. Kalidasan, V. *et al.* A guide in lentiviral vector production for hard-to-transfect cells,
824 using cardiac-derived c-kit expressing cells as a model system. *Scientific Reports* **11**, 1–
825 11 (2021).
826 57. Li, X. L. *et al.* A small protein encoded by a putative lncrna regulates apoptosis and
827 tumorigenicity in human colorectal cancer cells. *Elife* **9**, 1–44 (2020).
828 58. Suzuki, K., Bose, P., Leong-Quong, R. Y., Fujita, D. J. & Riabowol, K. REAP: A two
829 minute cell fractionation method. *BMC Research Notes* **3**, 294 (2010).
830 59. Holden, P. & Horton, W. Crude subcellular fractionation of cultured mammalian cell
831 lines. *BMC Research Notes* **2**, (2009).
832 60. Iwamura, T. *et al.* Induction of IRF-3/-7 kinase and NF-κB in response to double-
833 stranded RNA and virus infection: Common and unique pathways. *Genes to Cells* **6**, 375–
834 388 (2001).

61. Macdonald, S. J., Mostafa, H. H., Morrison, L. A. & Davido, D. J. Genome Sequence of Herpes Simplex Virus 1 Strain KOS. *Journal of Virology* **86**, 6371–6372 (2012).
62. Zhang, L. *et al.* NLRC3, a Member of the NLR Family of Proteins, Is a Negative Regulator of Innate Immune Signaling Induced by the DNA Sensor STING. *Immunity* **40**, 329–341 (2014).
63. Macdonald, S. J., Mostafa, H. H., Morrison, L. A. & Davido, D. J. Genome Sequence of Herpes Simplex Virus 1 Strain KOS. *Journal of Virology* **86**, 6371–6372 (2012).
64. Dobin, A. *et al.* STAR: Ultrafast universal RNA-seq aligner. *Bioinformatics* **29**, 15–21 (2013).
65. Kovaka, S. *et al.* Transcriptome assembly from long-read RNA-seq alignments with StringTie2. *Genome Biology* **20**, 1–13 (2019).
66. Ritchie, M. E. *et al.* Limma powers differential expression analyses for RNA-sequencing and microarray studies. *Nucleic Acids Research* **43**, e47 (2015).
67. Law, C. W., Chen, Y., Shi, W. & Smyth, G. K. voom: precision weights unlock linear model analysis tools for RNA-seq read counts. *Genome Biology* **15**, R29 (2014).
68. Korotkevich, G., Sukhov, V. & Sergushichev, A. Fast gene set enrichment analysis. Preprint of BioRxiv. *bioRxiv* (2019).
69. Wickham, H. Scales, axes and legends. in *ggplot2* 91–113 (Springer New York, 2009).
70. Gu, Z., Eils, R. & Schlesner, M. Complex heatmaps reveal patterns and correlations in multidimensional genomic data. *Bioinformatics* **32**, 2847–2849 (2016).
71. Leek, J. T., Johnson, W. E., Parker, H. S., Jaffe, A. E. & Storey, J. D. The SVA package for removing batch effects and other unwanted variation in high-throughput experiments. *Bioinformatics* **28**, 882–883 (2012).

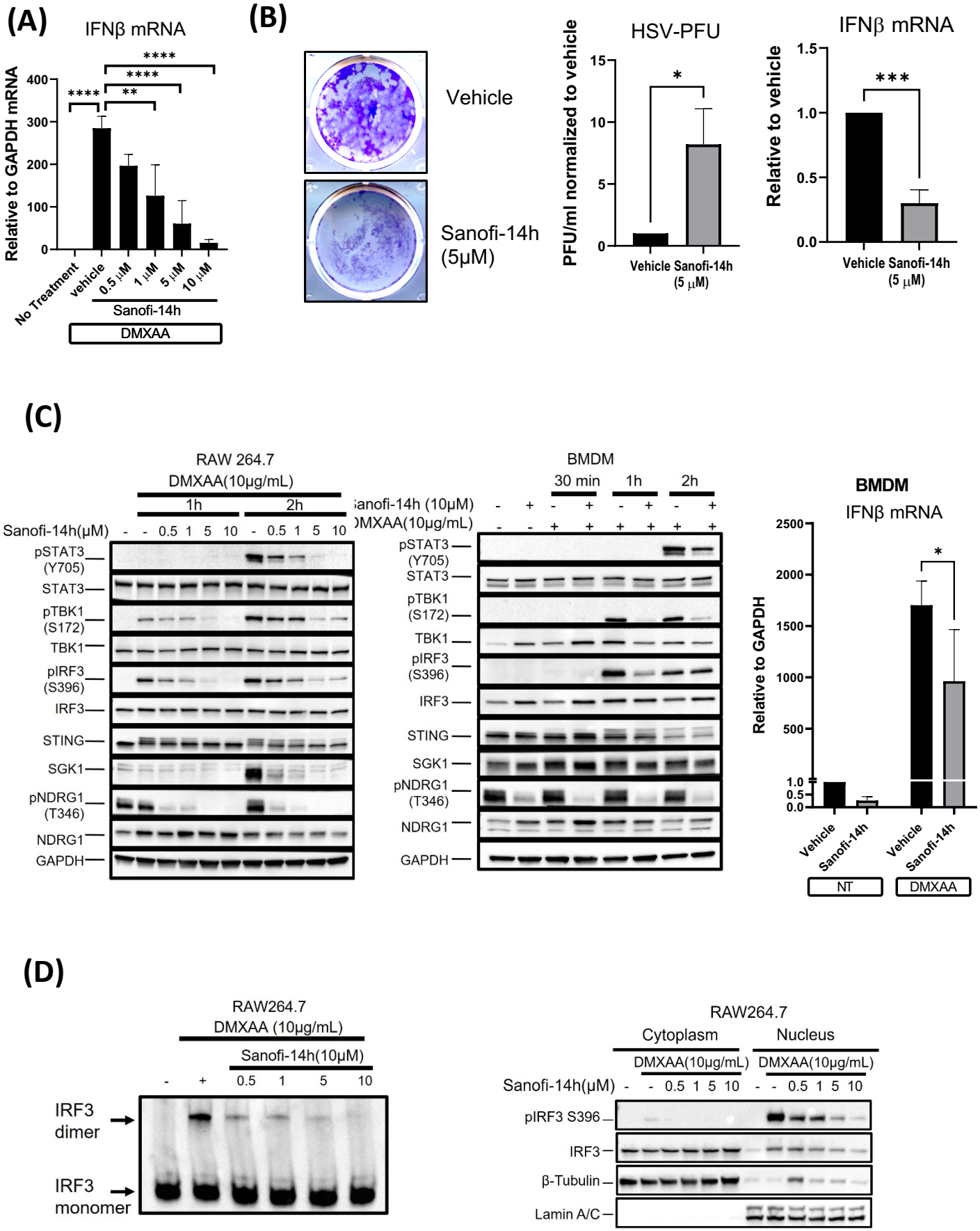
(A)
IFNβ mRNA
Relative to GAPDH mRNA
No Treatment
vehicle
0.5 μM
1 μM
5 μM
10 μM
Sanofi-14h
DMXAA
(B)
Vehicle
Sanofi-14h (5μM)
HSV-PFU
PFU/ml normalized to vehicle
Vehicle
Sanofi-14h (5 μM)
IFNβ mRNA
Relative to vehicle
(C)
RAW 264.7
DMXAA(10μg/mL)
1h
2h
Sanofi-14h(μM)
pSTAT3 (Y705)
STAT3
pTBK1 (S172)
TBK1
pIRF3 (S396)
IRF3
STING
SGK1
pNDRG1 (T346)
NDRG1
GAPDH
BMDM
30 min
1h
2h
Sanofi-14h (10μM)
DMXAA(10μg/mL)
BMDM
IFNβ mRNA
Relative to GAPDH
Vehicle
Sanofi-14h
NT
DMXAA
(D)
RAW264.7
DMXAA (10μg/mL)
Sanofi-14h(10μM)
IRF3 dimer
IRF3 monomer
RAW264.7
Cytoplasm
Nucleus
DMXAA(10μg/mL)
Sanofi-14h(μM)
pIRF3 S396
IRF3
β-Tubulin
Lamin A/C

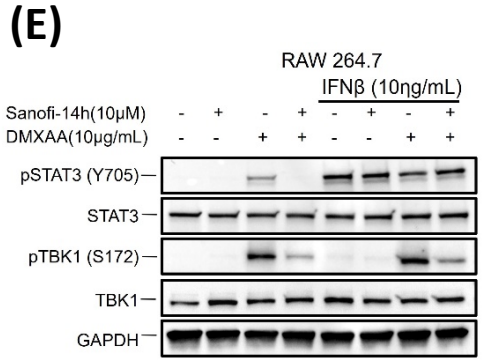


**Figure 1: SGK inhibitor Sanofi-14h impairs IFN expression and STING/TBK1/IRF3 signaling in macrophages**. **A)** RAW264.7 cells were pre-treated with Sanofi-14h at the indicated concentrations for 2 hours and then treated with DMXAA (10μg/mL) for an additional 2 hours. RT-qPCR IFNβ mRNA expression was normalized to the housekeeping gene GAPDH. **B)** Cells were seeded in 12 well plates and pre-treated the following day with Sanofi-14h (5 μM) for 24 h and then infected with HSV-1 KOS (MOI 0.1). The panel shows the plaque assay, and the graphs represents the PFU quantification (left) and FNβ mRNA after HSV-1 KOS infection(right). **C)** RAW264.7 macrophages (left panel) were plated in 60 mm plates and treated the next day with Sanofi-14h at the indicated doses for 2 h, followed by treatment with DMXAA (10μg/mL) for 1 and 2 h and immunoblotted. BMDM (right panel) were plated in the same way and treated with Sanofi-14h (10 μM) for 2 h and then with DMXAA (10μg/mL) for 30 min, 1 and 2 h. The graph shows the IFNβ mRNA expression normalized to GAPDH in BMDM. pNDRG1(T346) was a used a control to measure Sanofi-14h activity in both cell lines. **D)** Dimerization (left panel) and nuclear localization (right panel) of IRF3 after pre-treatment with Sanofi-14h at different doses for 2 hours and DMXAA for 1 hour. Lamin A/C and β-tubulin serve as control for the nuclear and cytoplasmic fractions, respectively. **E)** STAT3 phosphorylation under Sanofi-14h treatment, then with DMXAA and exogenous IFNβ treatment. After

921 pretreatment with and without Sanofi-14h (10 μM) for 2 hours, cells were treated with DMXAA
922 for either 2 h (control and control+Sanofi-14h) or 1 h and 45 min complemented with
923 exogenous IFNβ (10 ng/mL) for 15 min. At the end all DMXAA samples were treated for a total
924 of 2 h. BMDM: Bone Marrow Derived Macrophages, PFU: Plaque-Forming Unite, HSV: Herpes
925 Simplex Virus. Data are representative of three different experiments (* $p<0.05$).
926
927
928
929
930
931
932
933
934
935
936
937
938
939
940
941
942

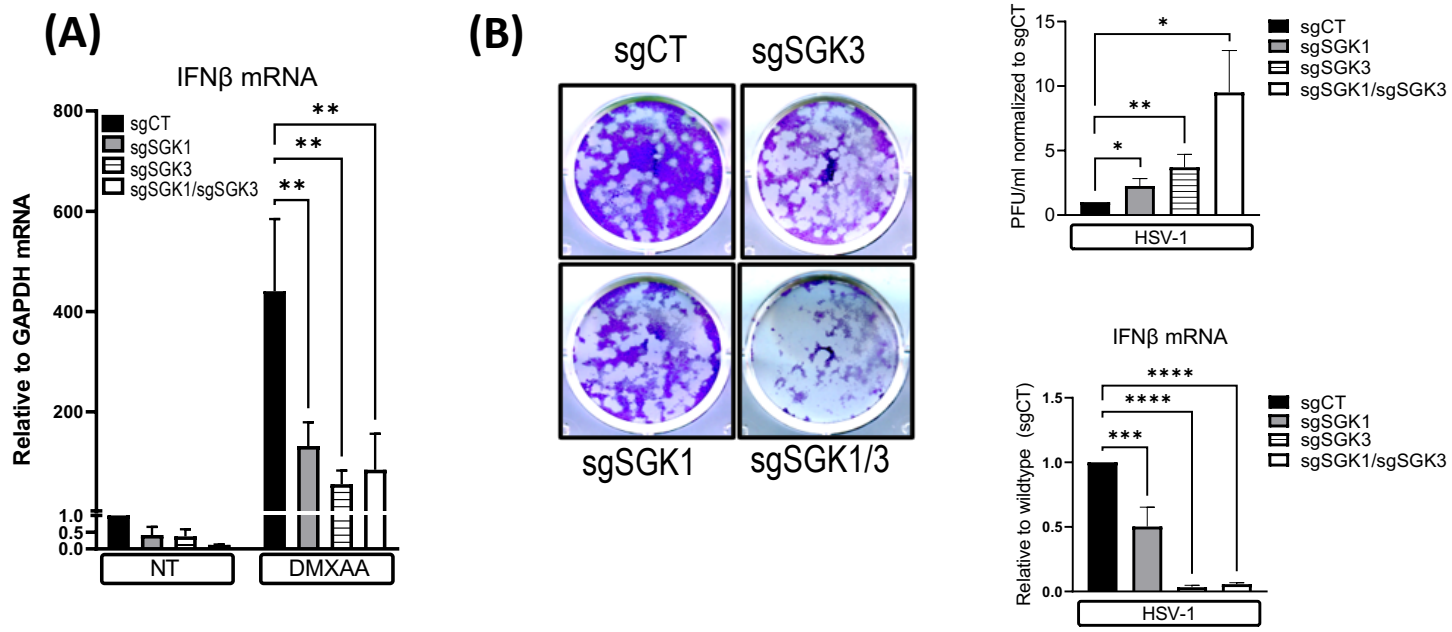
(A)
IFNβ mRNA
sgCT
sgSGK1
sgSGK3
sgSGK1/sgSGK3
Relative to GAPDH mRNA
800
600
400
200
1.0
0.5
0.0
**
**
**
NT
DMXAA
(B)
sgCT
sgSGK3
sgSGK1
sgSGK1/3
HSV PFU
PFU/ml normalized to sgCT
15
10
5
0
*
**
*
HSV-1
IFNβ mRNA
Relative to wildtype (sgCT)
1.5
1.0
0.5
0.0
****
****
***
HSV-1

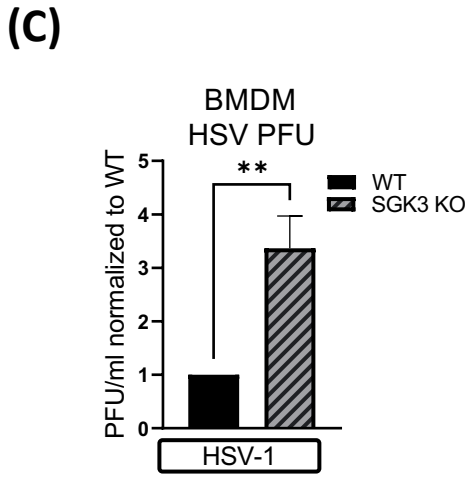
(C)
BMDM
HSV PFU
PFU/ml normalized to WT
5
4
3
2
1
0
**
WT
SGK3 KO
HSV-1

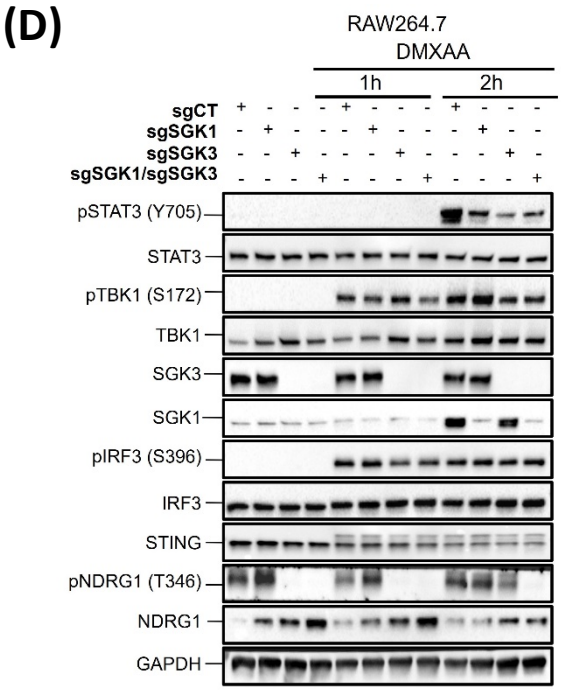
(D)
RAW264.7
DMXAA
1h
2h
sgCT
sgSGK1
sgSGK3
sgSGK1/sgSGK3
pSTAT3 (Y705)
STAT3
pTBK1 (S172)
TBK1
SGK3
SGK1
pIRF3 (S396)
IRF3
STING
pNDRG1 (T346)
NDRG1
GAPDH

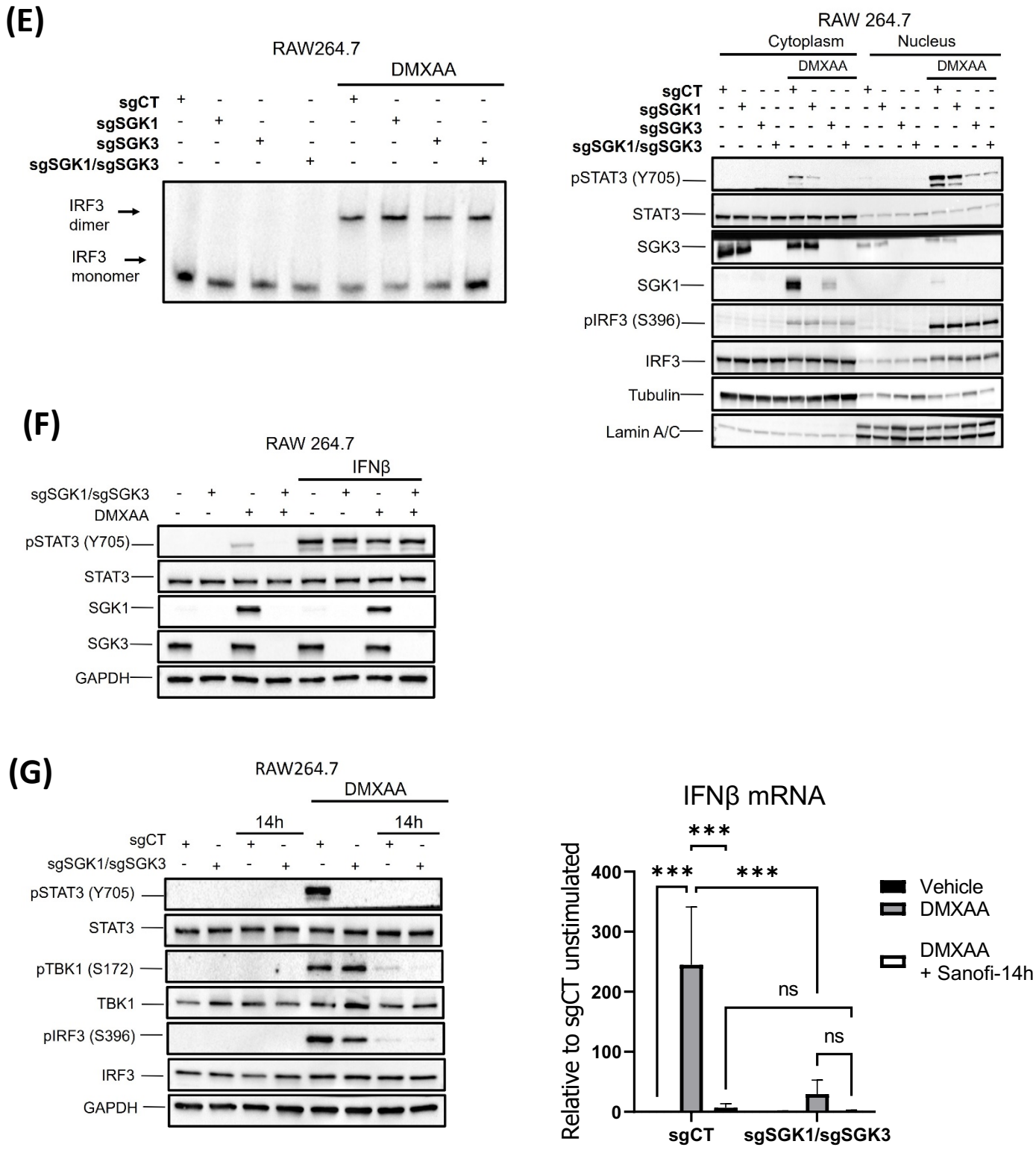


**Figure 2: SGK1/3 KO does not affect TBK1, IRF3 and STING phosphorylation but hinders IFNβ production and consequential STAT3 phosphorylation. A)** IFNβ mRNA expression in single and double(dKO) CRISPR generated RAW264.7 SGK1/3 KO cells with (top segment)

987 and without (bottom segment) DMXAA treatment for 2 h. **B)** RAW264.7 SGK KO cells were
988 plated in 12 well plates and infected with HSV-1 KOS. The upper panel shows the plaque
989 assay for single and dKO cells, whereas the upper right graph represents the PFU and lower
990 right graph shows IFNβ mRNA production in response to HSV infection these cells. **C)** PFU
991 after HSV infection in BMDM SGK3 KO cells. **D)** Cells were treated with DMXAA for 1 and 2 h
992 and then immunoblotted for different markers of activation. SGK1 and SGK3 protein levels
993 serve as evidence of the knock out and pNDRG1 function as a control for lost activity. **E)**
994 Dimerization (left panel) and nuclear localization (right panel) of IRF3 after DMXAA treatment
995 for 1 h in SGK single and dKO cells. Lamin A/C and β-tubulin serve as control for the nuclear
996 and cytoplasmic fractions, respectively. **F**) Immunoblot representing the treatment of SGK1/3
997 dKO cells with DMXAA (2 h total) with and without exogenous IFNβ (15 min). **G**) sgCT and
998 sgSGK1/sgSGK3 cells were treated with Sanofi-14h for 2 h and the treated with DMXAA for
999 an additional two hours before being immunoblotted for activation markers (left panel) and
1000 prepare for RT-qPCR (right graph) for IFNβ mRNA production. Data are representative of
1001 three different experiments (* $p<0.05$).
1002
1003
1004
1005
1006
1007
1008

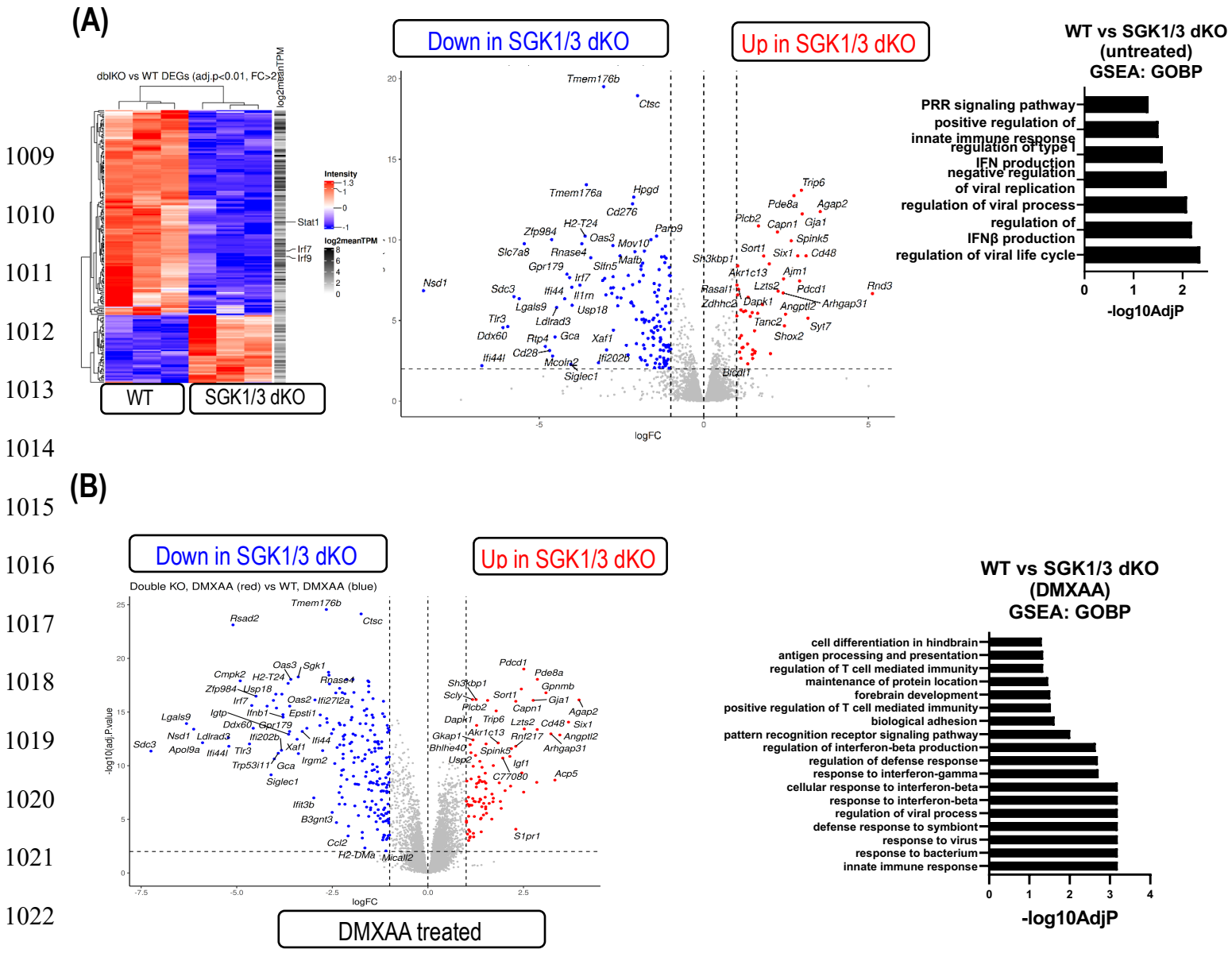
(A)
dblKO vs WT DEGs (adj.p<0.01, FC>2)
log2meanTPM
Intensity
Stat1
Irf7
Irf9
WT
SGK1/3 dKO
Down in SGK1/3 dKO
Up in SGK1/3 dKO
logFC
WT vs SGK1/3 dKO (untreated) GSEA: GOBP
PRR signaling pathway
positive regulation of innate immune response
regulation of type I IFN production
negative regulation of viral replication
regulation of viral process
regulation of IFNβ production
regulation of viral life cycle
-log10AdjP
(B)
Double KO, DMXAA (red) vs WT, DMXAA (blue)
-log10(adj.Pvalue)
logFC
DMXAA treated
WT vs SGK1/3 dKO (DMXAA) GSEA: GOBP
cell differentiation in hindbrain
antigen processing and presentation
regulation of T cell mediated immunity
maintenance of protein location
forebrain development
positive regulation of T cell mediated immunity
biological adhesion
pattern recognition receptor signaling pathway
regulation of interferon-beta production
regulation of defense response
response to interferon-gamma
cellular response to interferon-beta
response to interferon-beta
regulation of viral process
defense response to symbiont
response to virus
response to bacterium
innate immune response
-log10AdjP
(C)
sgCT
sgSGK1/sgSGK3
sgCT (DMXAA)
sgSGK1/sgSGK3(DMXAA)
mRNA TPM
Irf1
Irf2
Irf3
Irf5
Irf7
Irf8
Irf9
Irf4
Irf6
ns

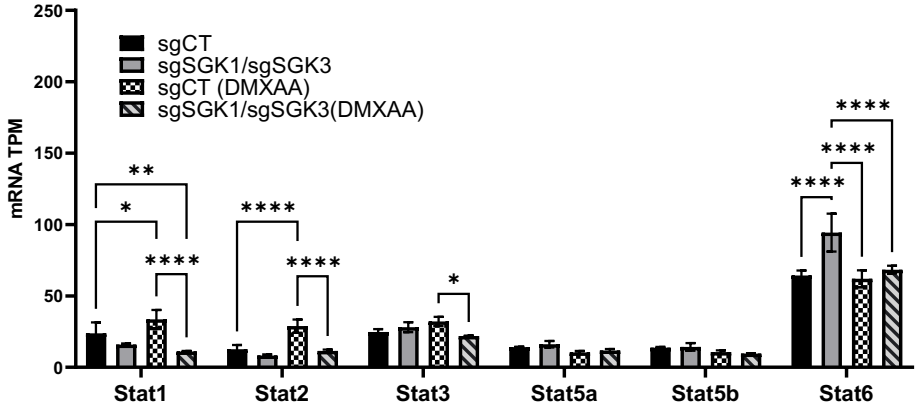
sgCT
sgSGK1/sgSGK3
sgCT (DMXAA)
sgSGK1/sgSGK3(DMXAA)
mRNA TPM
250
200
150
100
50
0
**
*
****
****
****
*
****
****
****
Stat1
Stat2
Stat3
Stat5a
Stat5b
Stat6

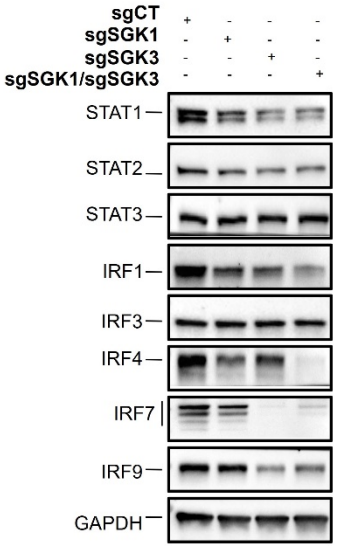
sgCT
sgSGK1
sgSGK3
sgSGK1/sgSGK3
STAT1
STAT2
STAT3
IRF1
IRF3
IRF4
IRF7
IRF9
GAPDH

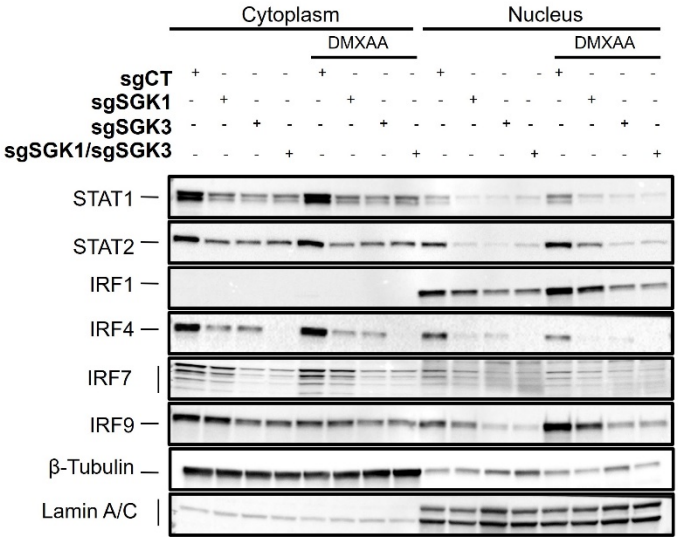
Cytoplasm
Nucleus
DMXAA
DMXAA
sgCT
sgSGK1
sgSGK3
sgSGK1/sgSGK3
STAT1
STAT2
IRF1
IRF4
IRF7
IRF9
β-Tubulin
Lamin A/C

**(D)**

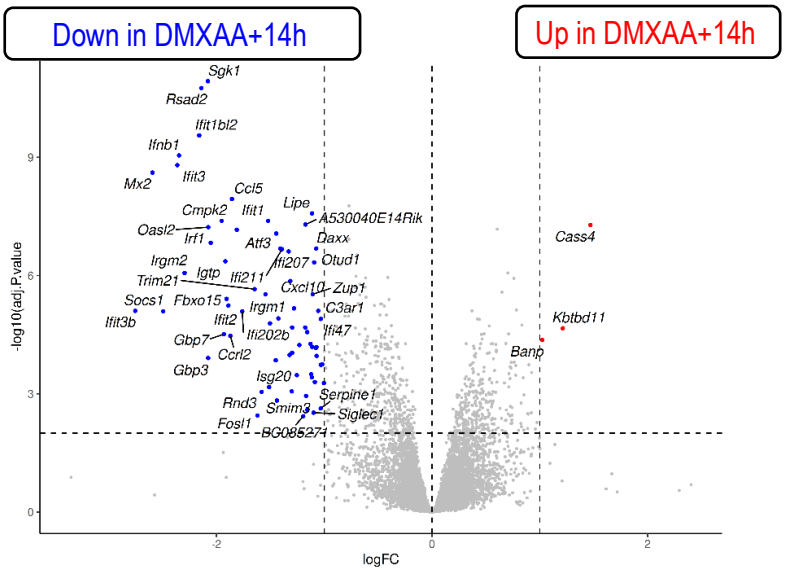
Down in DMXAA+14h
Up in DMXAA+14h
-log10(adj.P.value)
logFC
Sgk1
Rsad2
Ifit1bl2
Ifnb1
Ifit3
Mx2
Ccl5
Cmpk2
Ifit1
Lipe
A530040E14Rik
Oasl2
Irf1
Atf3
Daxx
Irgm2
Ifi207
Otud1
Trim21
Igtp
Ifi211
Cxcl10
Zup1
Socs1
Fbxo15
Irgm1
C3ar1
Ifit3b
Ifit2
Ifi47
Gbp7
Ifi202b
Ccrl2
Gbp3
Isg20
Serpine1
Rnd3
Smim3
Siglec1
Fosl1
BC085271
Cass4
Kbtbd11
Banp

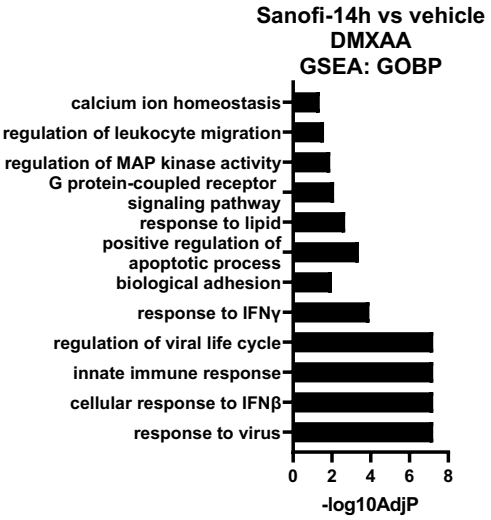
Sanofi-14h vs vehicle
DMXAA
GSEA: GOBP
calcium ion homeostasis
regulation of leukocyte migration
regulation of MAP kinase activity
G protein-coupled receptor signaling pathway
response to lipid
positive regulation of apoptotic process
biological adhesion
response to IFNγ
regulation of viral life cycle
innate immune response
cellular response to IFNβ
response to virus
0
2
4
6
8
-log10AdjP

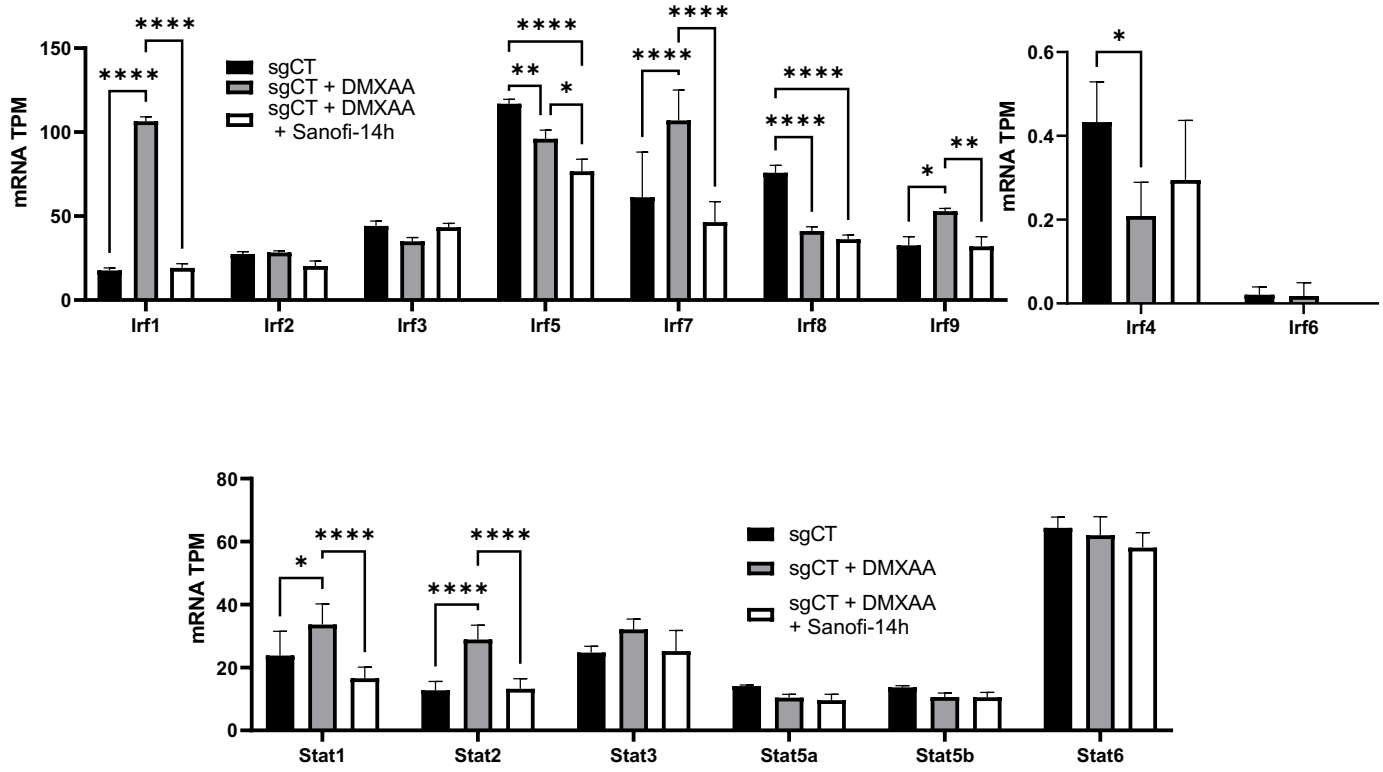


**Figure 3: SGK1 and SGK3 KO blocks expression of Interferon Stimulated Genes (ISGs) and innate immunity regulators. A)** Heatmap (left panel) reflecting the differentially expressed genes after knocking out SGK1/3 without any stimulation. Blue indicates genes that are being downregulated while red show genes that are upregulated in the dKO cells. Volcano plot (middle graph) depicting the expression of Interferon Stimulated Genes (ISGs) at basal levels in SGK1/3 dKO cells plotted by log fold change(logFC) in the x-axis and -log of adjusted p value in the y-axis. Right graph depicts the Gene Set Enrichment Analysis (GSES) and Gene Ontology Biological Process (GOBP) representing the most changes pathways after SGK1/3 dKO in non-stimulated cells based on -log10 of the adjusted p value in the x-axis. **B)** Volcano plot (left graph) showing the expression of ISGs after DMXAA treatment for 2 h in SGK1/3 dKO cells. Significance was achieved with an adjusted p value of <0.05 and a fold change >2 in either direction. GSES and GOBP analysis (right graph) of the most affected pathways after

1075 DMXAA treatment in SGK1/3 dKO cells. **C)** IRFs and STATs mRNA expression in Transcripts
1076 Per Million (TPM) (*p<0.05) in SGK1/3 dKO cells with and without DMXAA(2h). Immunoblot of
1077 IRFs and STATs protein expression at basal conditions (left panel) and their nuclear
1078 localization (right panel) after DMXAA treatment for 1h. **D)** Volcano plot (left graph) showing
1079 genes that are upregulated (red) and downregulated (blue) by Sanofi-14h on the DMXAA
1080 response in RAW264.7 cells. GSES and GOBP analysis (right graph) reflecting the effects of
1081 Sanoni-14h on the most significant DMXAA responsive pathways. IRFs and STATs mRNA-
1082 TPM expression with and without Sanofi-14h after DMXAA treatment. All experiments were
1083 repeated at least three times.
1084
1085
1086
1087
1088
1089
1090
1091
1092
1093
1094
1095
1096

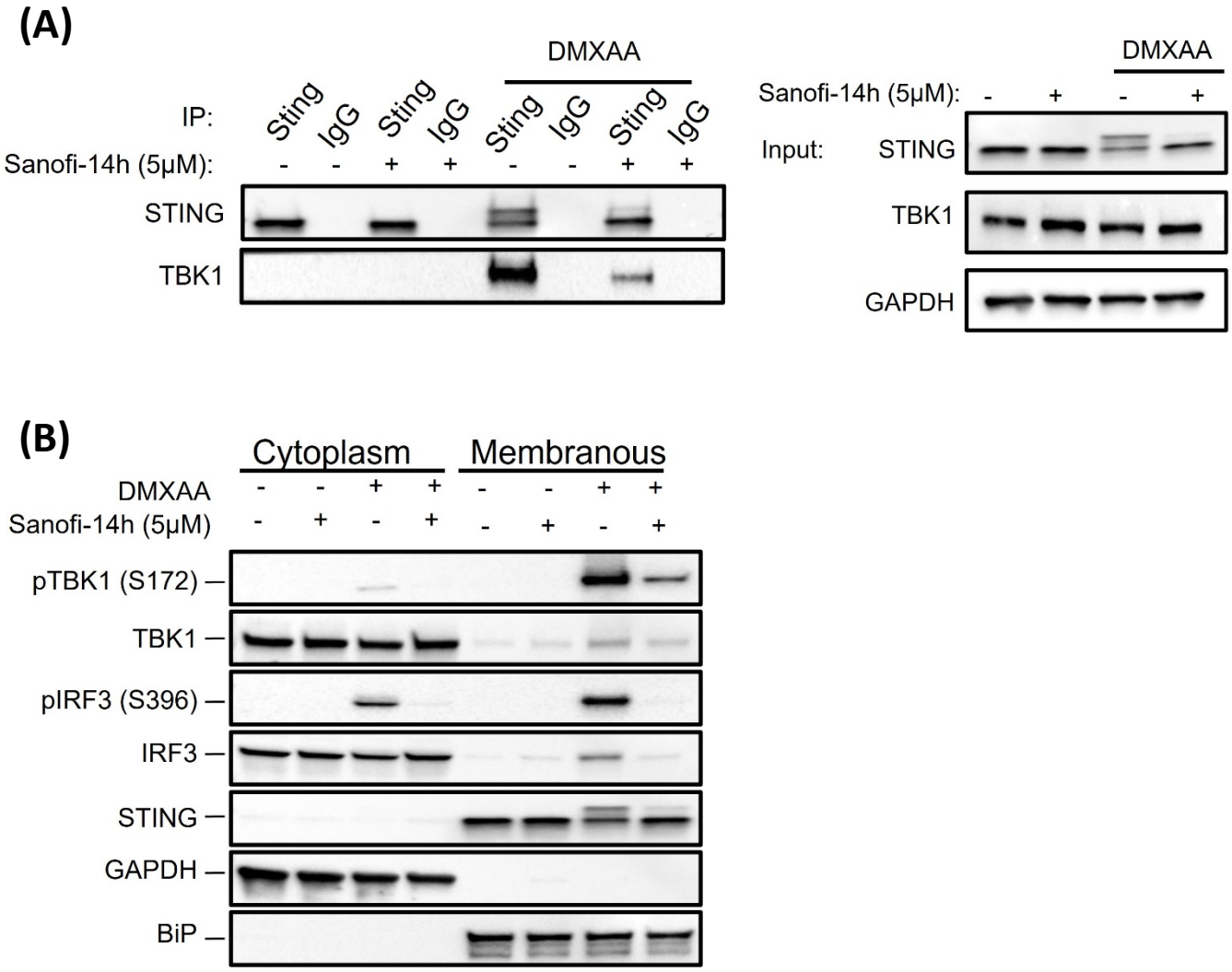


**Figure 4: Sanofi-14h disrupts TBK1/STING interaction. A)** Effects of Sanofi-14h treatment on STING and TBK1 interaction of DMXAA treatment for 1h. STING was immunoprecipitated and the interaction was measured based on TBK1 detection in immunoblot. IgG was used a negative control and inputs show the levels of both proteins in total lysate. **B)** RAW264.7 cells were fractionated and immunoblotted for TBK1 and IRF3 translocation into the ER-Golgi Space after Sanofi-14h(2h) and DMXAA treatment for 1h.

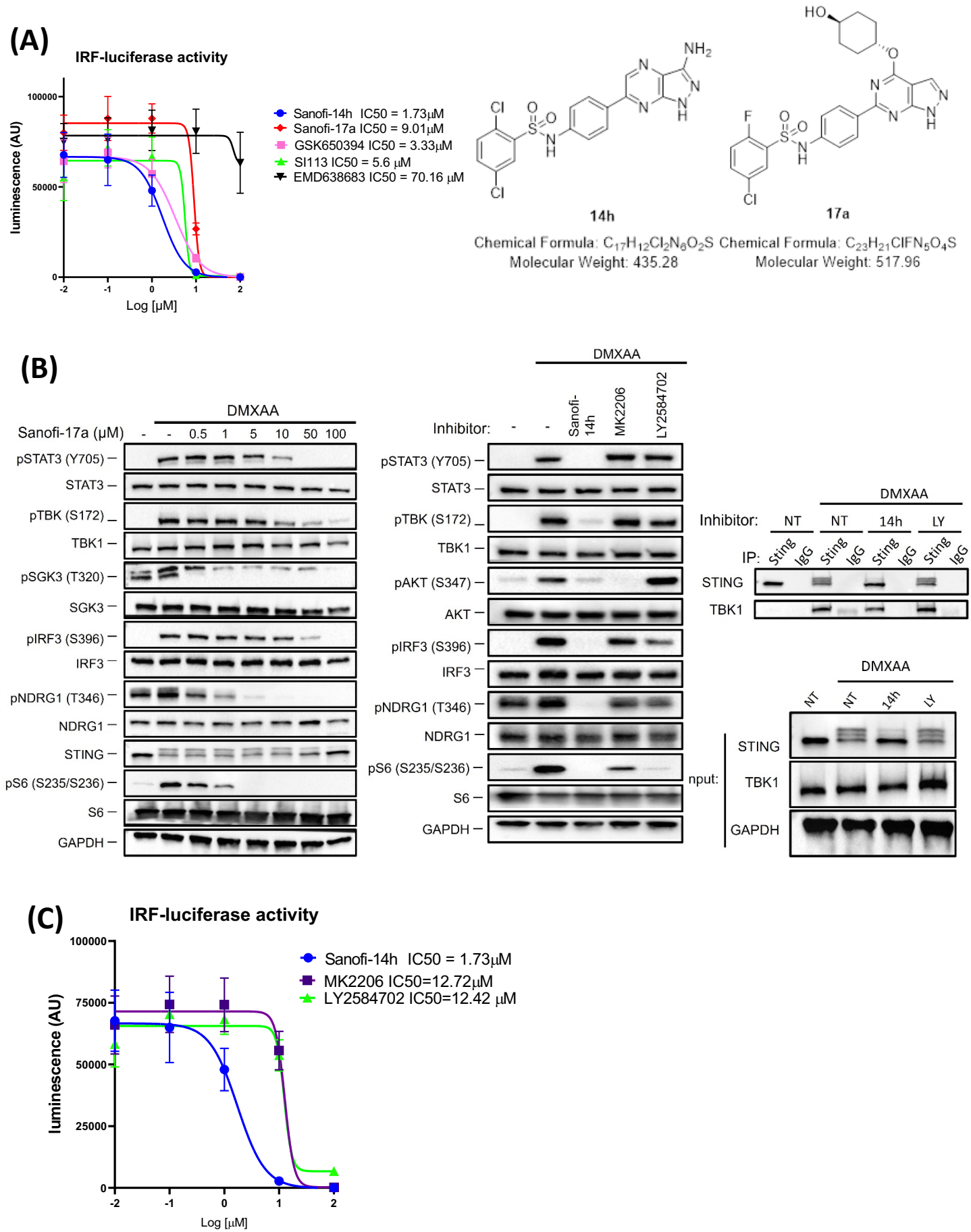
(A)
IRF-luciferase activity
luminescence (AU)
Log [μM]
Sanofi-14h IC50 = 1.73μM
Sanofi-17a IC50 = 9.01μM
GSK650394 IC50 = 3.33μM
SI113 IC50 = 5.6 μM
EMD638683 IC50 = 70.16 μM
14h
Chemical Formula: C17H12Cl2N6O2S
Molecular Weight: 435.28
17a
Chemical Formula: C23H21ClFN5O4S
Molecular Weight: 517.96
(B)
DMXAA
Sanofi-17a (μM)
pSTAT3 (Y705)
STAT3
pTBK (S172)
TBK1
pSGK3 (T320)
SGK3
pIRF3 (S396)
IRF3
pNDRG1 (T346)
NDRG1
STING
pS6 (S235/S236)
S6
GAPDH
Inhibitor:
Sanofi-14h
MK2206
LY2584702
pAKT (S347)
AKT
IP:
Sting
IgG
NT
14h
LY
(C)
IRF-luciferase activity
luminescence (AU)
Log [μM]
Sanofi-14h IC50 = 1.73μM
MK2206 IC50=12.72μM
LY2584702 IC50=12.42 μM

1140 **Figure 5: Other SGK inhibitors have variable effect on IRF DMXAA driven activation. A)**
1141 IRF activation luciferase assay (left graph) in the presence of diverse SGK inhibitors and
1142 DMXAA stimulation. Raw-Dual Luciferase cells were seeded in 96 well plates, left to rest
1143 overnight and treated with the different inhibitors at different doses for 2 h and then treated
1144 with DMXAA for 24h. Luciferase signal directly correlates with type I production and the graph
1145 depict Log10 of the drug concentrations. Chemical Structure of Sanofi-14h and closely related
1146 compound Sanofi-17a (right panel). **B)** Immunoblots (left panel) showing the effects of Sanofi-
1147 17a, LY258702 and MK2206 on markers after DMXAA treatment. Cells were treated with
1148 different doses of Sanofi-17a and with 10 μM of Sanofi-14h, MK2206 and LY2584702 for 2 h
1149 and the treated with DMXAA for two additional hours. Co-immunoprecipitation (right panel)
1150 showing the effects of LY258702(2 h pre-treatment) on TBK1/STING interaction after DMXAA
1151 treatment for 1 h. **C)** Dual Luciferase assay depicting the effects of the same inhibitors on
1152 IFNβ production. The graph is depicted the same way as **A.**
1153
1154
1155
1156
1157
1158
1159
1160
1161

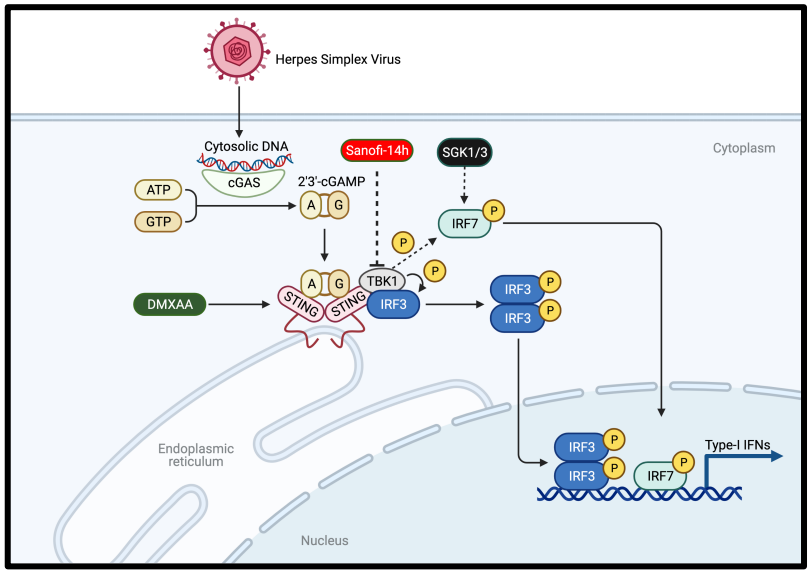


Adapted from "cGAS detects Cytosolic dsDNA", BioRender.com (2022), https://app.biorender.com/biorender-templates

**Figure 6: Model of SGK regulation of STING/TBK1 signaling**. Sanofi-14h inhibits phosphorylation of TBK1 through an unknown mechanism preventing STING and IRF3 phosphorylation, dimerization and nuclear translocation in the presence of 2'3'-cGAMP and DMXAA. SGK1 and SGK3 promote IRF7 expression and stabilization under basal and DMXAA stimulated conditions in macrophages.

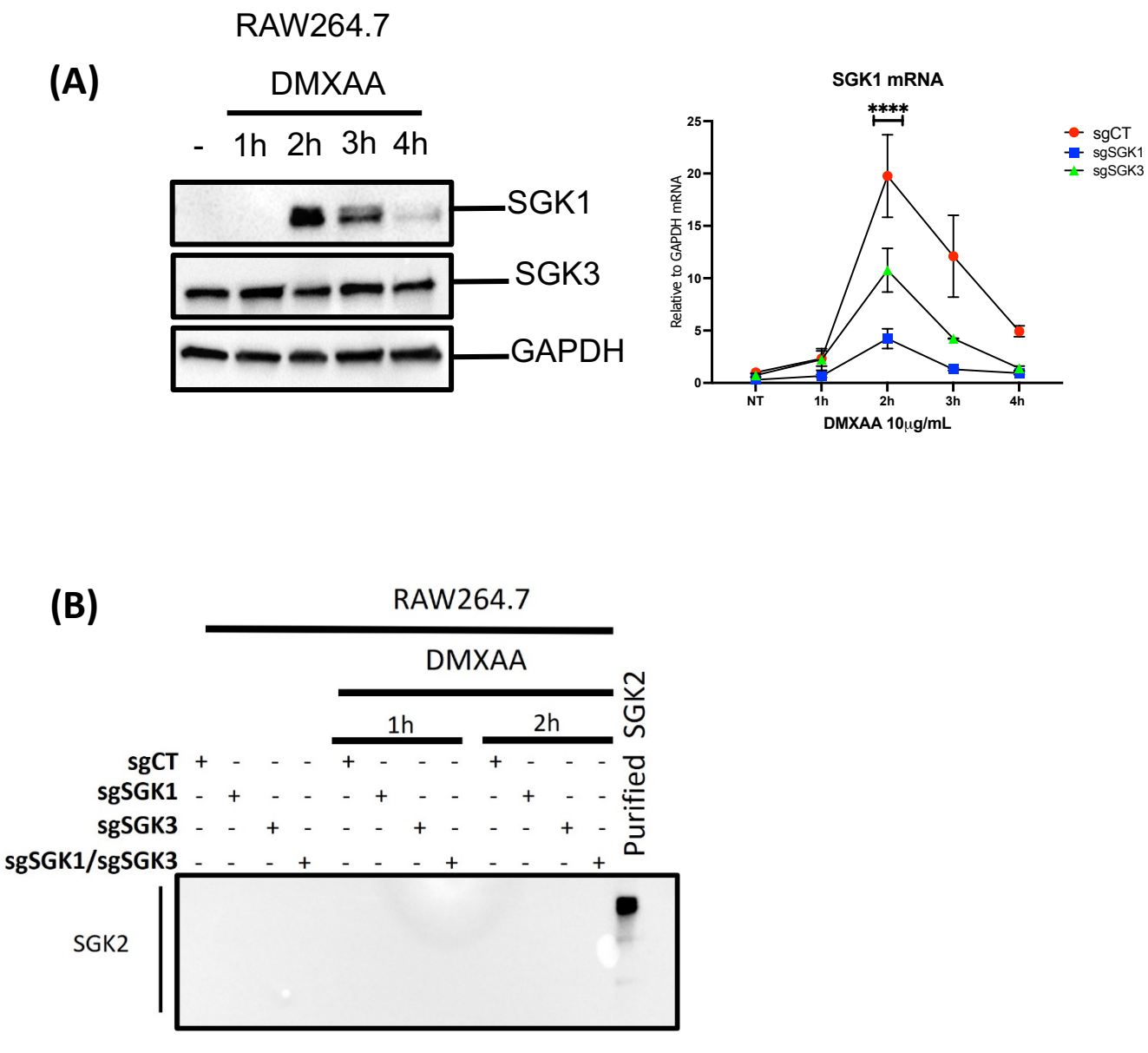


**Supplemental figures: A)** DMXAA increases mRNA and protein expression of SGK1, but not SGK3 through time. Upper Immunoblot shows the levels of SGK1 protein and left graph depicts the SGK1 mRNA levels after DMXAA treatment at different times in SGK1 and SGK3 single KO cells. **B)** SGK2 is not expressed in RAW264.7 cells at basal or after DMXAA treatment at the protein(immunoblot) or mRNA levels (data not shown).